1985

Contactless resistance measurement systems for gallium arsenide /

Michael Paul Petroski
Lehigh University

CONTACTLESS RESISTANCE MEASUREMENT SYSTEMS FOR GALLIUM ARSENIDE

by

Michael Paul Petroski

A Thesis

Presented to the Graduate Committee

of Lehigh University

in Canadacy for the Degree of

Master of Science

in

Electrical Engineering

This thesis is accepted and approved in partial

fulfillment of the requirements for the degree of

Master of Science

in

Electrical Engineering

9/18/85

(date)

Douglas Frey

Professor in Charge

Lee D. Thompson

Chairman of Department

ACKNOWLEDGMENT

I wish to thank Professor Doug Frey for his support and guidance both electrically and otherwise, for the many pep-talks when I was down, and for the beers we shared.

This thesis is dedicated to the Stouts: Mike, Elaine, Katie and Ed, who welcomed me into their home and made me part of their family. Your kindness and love will always be remembered.

Table of Contents

TABLE OF FIGURES

Abstract

This thesis will discuss three methods to determine resistivity of semiconductors contactlessly. The methods include loading resonant circuits, using quadrature detection, and using an LCR meter that provides capacitance and dissipation data. The circuit diagrams, mathematics, and results are presented for each method. The resonant circuits and quadrature detection methods showed limited success in the resistivity range of silicon. The LCR method showed the greatest potential as a technique to determine resistivity of GaAs in the 10^{7} to 10^{9} ohm-cm range.

INTRODUCTION

It is expected that the next generation computers will rely heavily on gallium-arsenide devices to achieve blinding speeds. The high speeds are possible because electrons in GaAs have an effective mass of 0.068 times that of their actual mass. Power dissipation per gate is the same as for silicon, but gates made of GaAs are ten times faster. Operating temperatures from -200 to +200 C along with radation hardness of 10^8 RADS make GaAs attractive to military and space applications.

Before devices can be fabricated on GaAs, the resistivity (among other parameters) must be known. The present method for determining the resistivity involves a four point probe that touches the virgin semiconductor. As would be expected, such intimate contact renders the wafer unsuitable for device fabrication. The relative inexperience of making GaAs as opposed to silicon prevents destructively testing random samples to qualify an entire batch. The need for a contactless resistivity measurement system seems apparant.

This thesis will discuss three approaches to contactlessly determine the resistivity of GaAs. All three

methods use a capacitance probe to look into the semiconductor. The first method uses the probe to load an LC tank operating at radio frequencies. A measurement of the power required to maintain oscillation is related to the conductivity of the sample on the probe. The second method uses quadrature detection to determine the real (in phase) componant of a signal passed through the probe. The final method uses the values of dissipation and capacitance given by an HP LCR meter to determine the resistivity of the probe-GaAs set up. Although none were entirely successful for samples in the 10^{7} -10^{9} cm range, this discussion may provide some insight for future work.

CHAPTER ONE

Semiconductor Measurement using Resonant Circuits

Miller, Robinson and Wiley demonstrated a contactless semiconductor measurement system exhibiting 1% linearity, 100:1 range and limiting sensitivity of 10^{-5} mho/square. Their technique involved monitoring the power required to maintain a fixed oscillation as the quality factor of a resonant circuit is degraded. The circuit involves a 10 MHz inductor-capacitor resonant tank with the inductor as shown below.

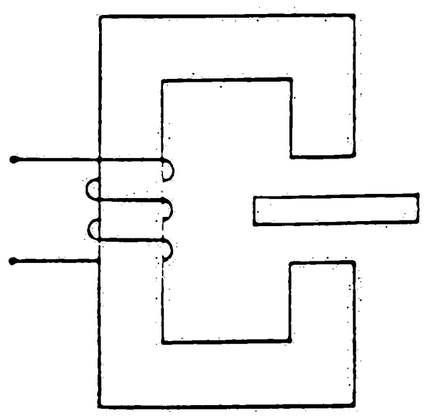

Semiconductors inserted into the gap experience Joule heating due to eddy currents induced by the oscillating magnetic field. The power absorbed by the semiconductor is directly proportional to its conductivity. Automatic Gain Control (AGC) circuitry maintains the set amplitude of oscillation. The current driven into the tank is proportional to the power absorbed, and thus to the conductivity of the semiconductor.

Figure 1.1 is a schematic of a circuit similar to the one described above. The inductor is a standard air core inductor. The Q was degraded by soldering resistors in parallel with the inductor and capacitor. A graph of the voltage out of the AGC part of the circuit as a function of the conductance of the resistors soldered in place is Figure 1.2 . A fairly linear relationship was observed for resistors up to 10 KΩ. Resistors greater than 10 KΩ did not appreciably change the DC output. This was due to the relatively low Q of the parallel RLC tank. A circuit with a large Q would be more sensitive to slight loadings (large resistors) . Also noticed were frequency shifts as large as 100 kHz. Since the Q of a circuit is a function of the signal frequency, an oscillator that changes frequency for different loading should show significant error built in. The desire for a fixed frequency oscillator with a high Q led to simply replacing the LC tank by a quartz crystal. That circuit would not oscillate.

Modulation Technique to Determine Resistivity

Quartz Crystal

Trying a different approach, an oscillator that modulated the signal going to a quartz crystal was developed. A quartz crystal is modeled as shown below.

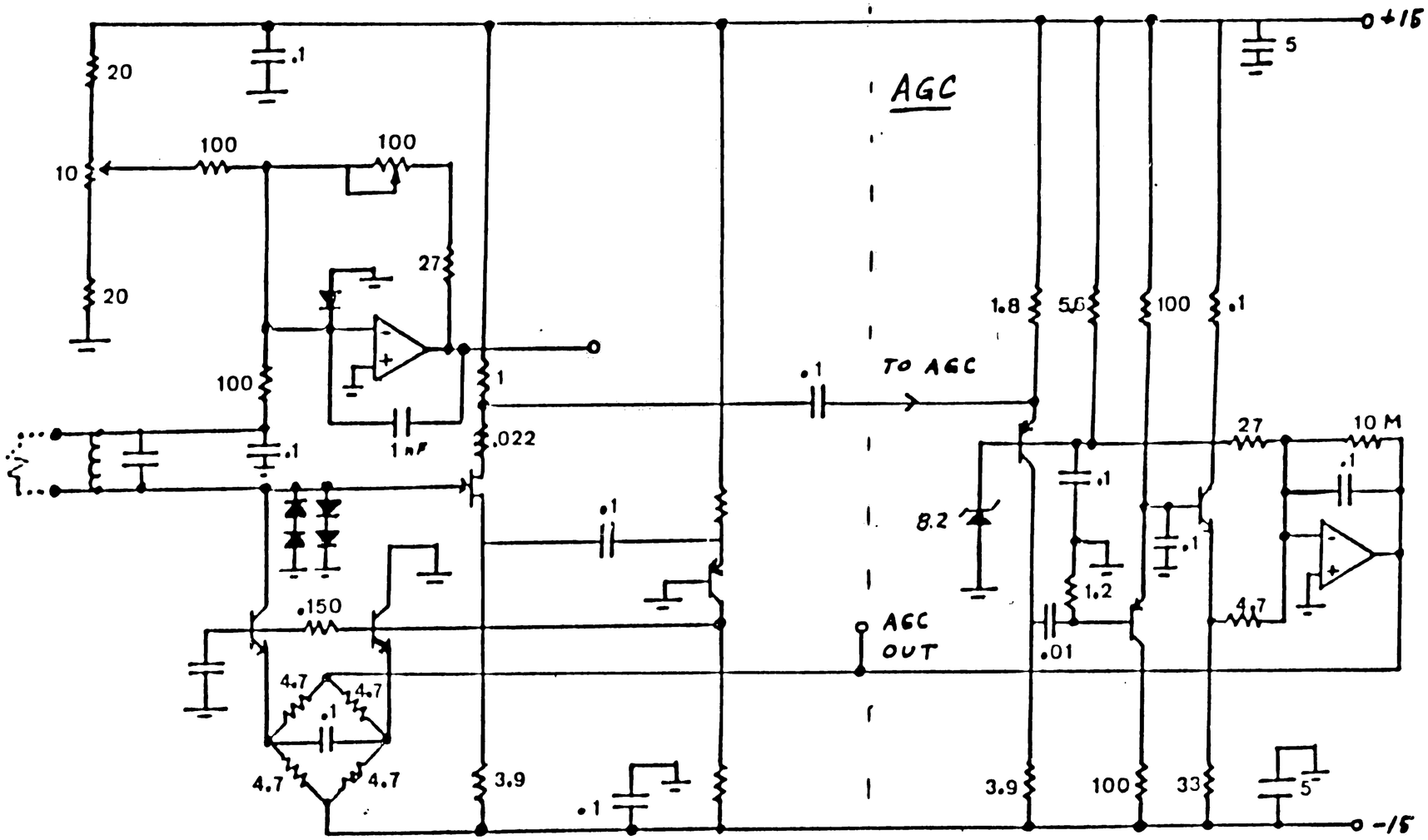

ALL RESISTORS KΩ

ALL CAPACITORS μF

Figure 1.1 Oscillator with AGC

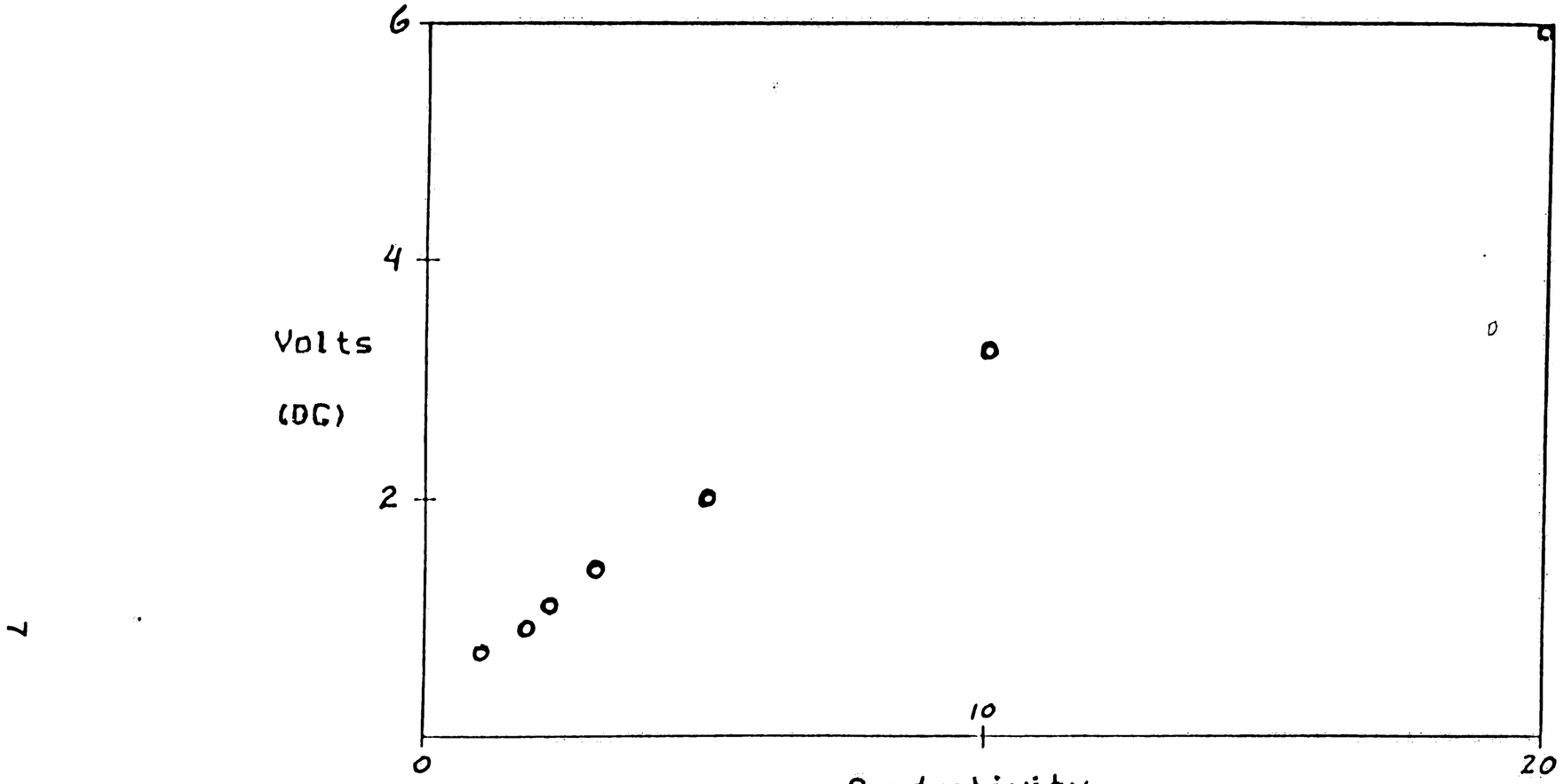

Figure 1.2 Graph of Output Voltage from AGC

vs

Conductivity of Resistors

in Parallel with the

LC Tank

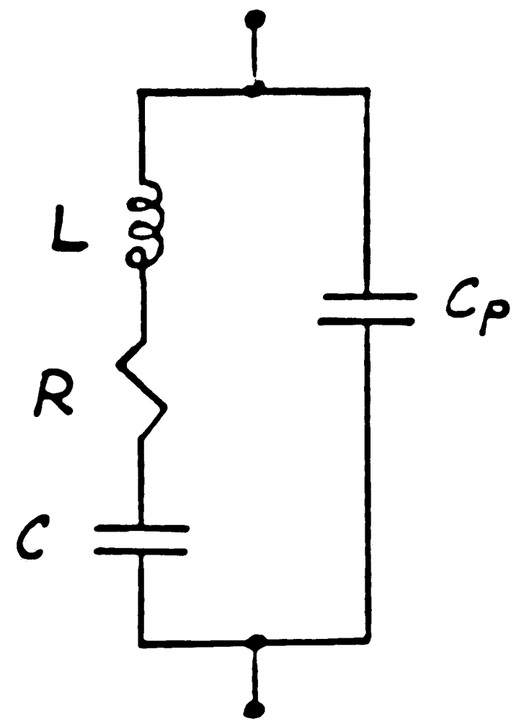

Cp is due to the crystal holder and is on the order of pico-Farads. C is on the order of 0.01 pico-Farads. L is typically a few Henries and R is on the order of Kilo-ohms. The impedance of the model is

$$Z = \frac{s^2 LC + s RC + 1}{s(s^2 LC\,Cp + s RC\,Cp + Cp + C)} \qquad (1.1)$$

There are two frequencies of interest; when the numerator is minimum (called series resonance) and when the denominator is minimum (parallel resonance).

Series Resonance

Setting the numerator equal to zero gives

$$s^2 (LC) + s (RC) + 1 = 0$$

The quadratic formula gives

$$s = \frac{-R}{2L} \pm \frac{\sqrt{(RC)^2 - 4LC}}{2LC}$$

Since an oscillatory term is desired, complex conjugate roots are expected. This forces

$$4LC > (RC)^2$$

If we let

$$4LC >> (RC)^2$$

(which is reasonable for the orders of values given), then the frequency of interest is

(1.2) $$w = \frac{1}{\sqrt{LC}}$$

Putting this value into the impedance equation indicates the impedance in the series mode is

(1.3) $$Z = R$$

Parallel Resonance

The second mode of interest is the parallel mode. That occurs when the denominator approaches zero. The case when s = 0 is trivial. The other roots are as below.

$$s^2 (LC\ Cp) + s (RC\ Cp) + (Cp + C) = 0$$

The quadratic formula gives

$$s = \frac{-R}{2L} \pm \frac{\sqrt{(RC\ Cp)^2 - 4LC(Cp + C)}}{2LC\ Cp}$$

Again complex conjugates are desired. This requires

$$4LC\ Cp(Cp + C) > (RC\ Cp)^2$$

It is acceptable to let

$$4LC\ Cp(Cp + C) >> (RC\ Cp)^2$$

The w of interest is now

$$w = \frac{\sqrt{(Cp + C)}}{\sqrt{LC\ Cp}} \qquad (1.4)$$

Although Cp >> C, it can not be removed from the expression for w in the parallel mode (if it were, the parallel mode would equal the series mode). Putting the value for the frequency of the parallel mode back into the impedance equation gives

$$Z = \frac{\frac{C}{Cp} - j\ R\sqrt{\frac{C}{L}}}{\frac{(Cp+C)}{L} R} \qquad (1.5)$$

Since the imaginary part is relatively small,

$$Z = \frac{C\ L}{Cp(Cp + C)R} \qquad (1.5a)$$

Values for a standard 400 KHz quartz crystal are as follows:

L=3.1 H

C=0.05 pF

Cp=6.0 pF

R=4.0 KΩ

Using these values in equations 1.2 and 1.4 shows the parallel resonant frequency at 399.54 KHz and the series resonant frequency at 397.89 KHz. The impedance at parallel resonance is approximately 1.1 MΩ and the impedance at series resonance is 4.0 KΩ by way of equations 1.5 and 1.3. Note that the series impedance is lower than the parallel impedance (as expected).

Modulating Oscillator

The oscillator that uses the quartz crystal is Figure 1.4 . Figure 1.3 shows a block diagram of the oscillator. The transfer function of the quartz crystal is the block labeled H(w). The V-I converter is realized by the FET and three bipolar transistors in the lower center of the schematic. The FET drain current is essentially Va/1K. Most of the AC drain current leaves the source, through the .1 uF capacitor and into the low impedance of the NPN emitter below the .1 uF capacitor at the center. The two NPN's below it act as a current mirror sourcing the current from the two emitters tied together at the right of the 3086

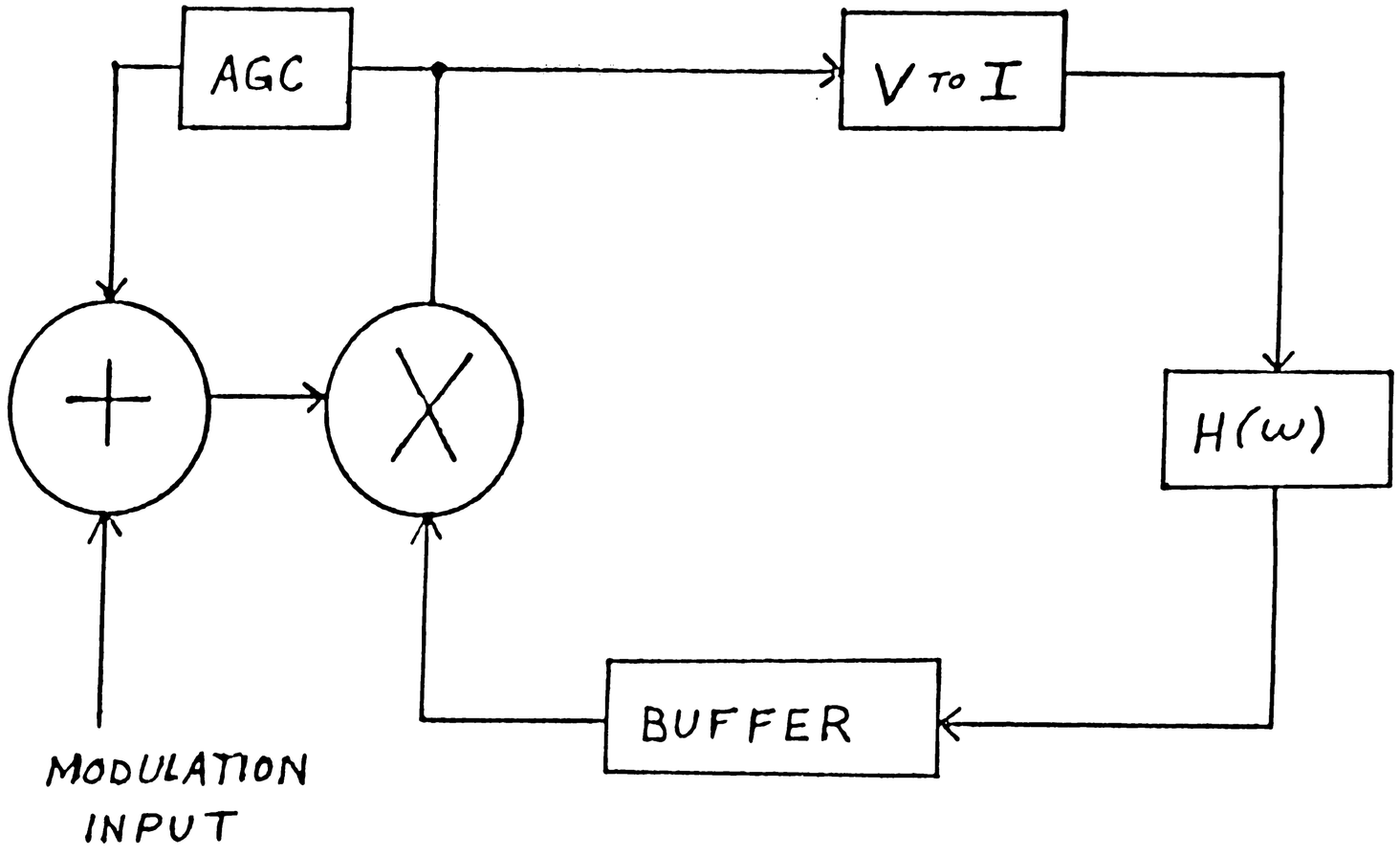

Figure 1.3 Block Diagram of Modulating Oscillator with AGC

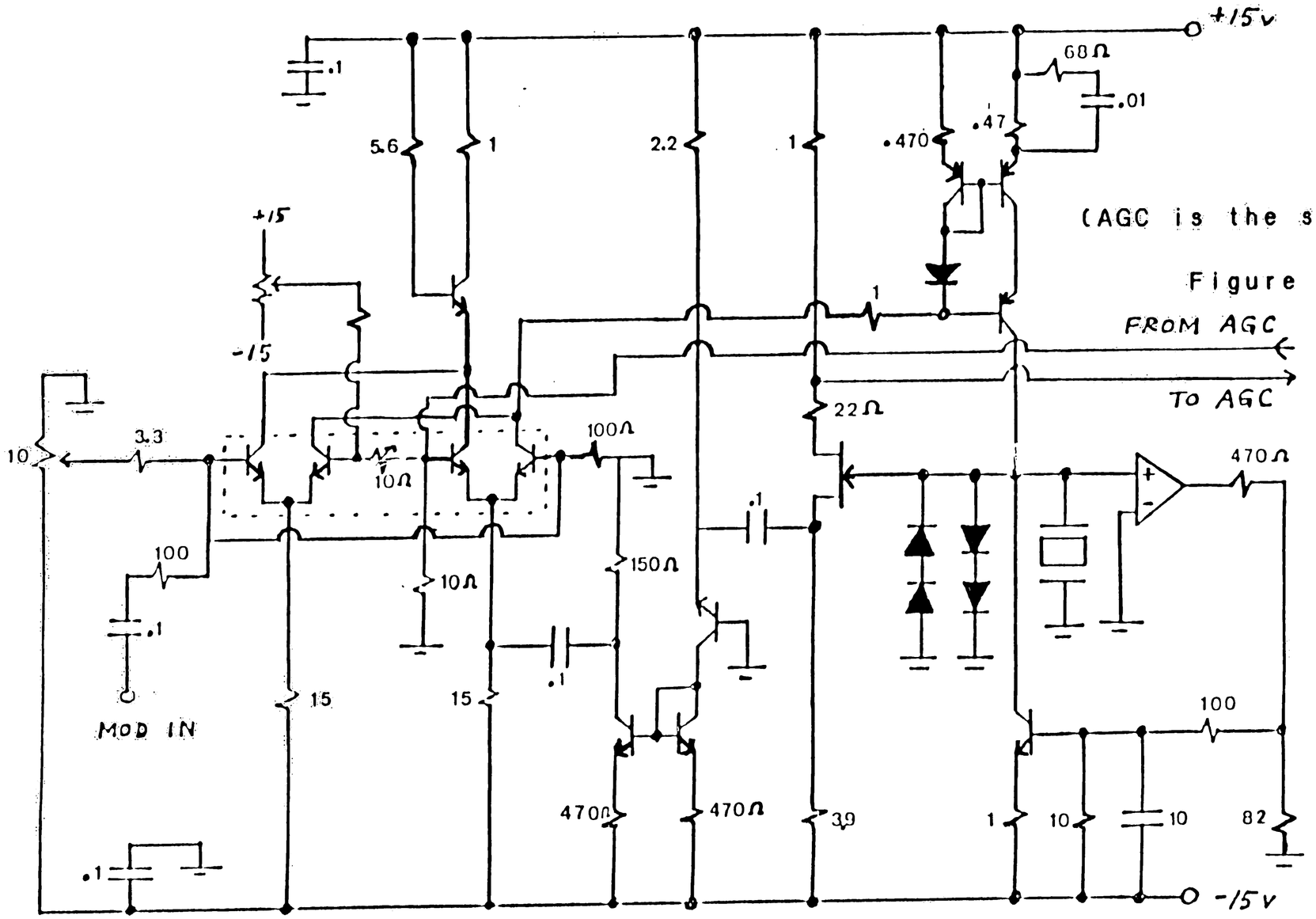

(AGC is the same as AGC of Figure 1.1)

ALL RESISTORS KΩ
ALL CAPACITORS μF

Figure 1.4 Schematic of Modulating Oscillator with AGC

and the 150Ω resistor to ground. Assuming that the dynamic impedance of the emitter pair is 25Ω (considering the DC bias current), by current division the AC current out of the pair is:

$$Iac = .857\ Va/1k$$

The four transistors of the 3086 are connected as a multiplier. Note that the outside bases are at the same potential determined by the 10K potentiometer tap position. The inside bases are also at a common potential determined by the AGC circuit output and oscillator input. Pot P2 adds a small offset to counteract the random differential pair input offset voltage. Since the bases of the four transistors are at similar potentials close to ground, both differential pairs experience the same DC bias tail current. The tail current in the right differential pair is given by

$$(Idc + Iac)$$

The current flowing in the right collector of this pair is

$$G(Idc + Iac)$$

where G is a fraction determined by the base to base bias of the pair. We assume large transistor current gain in the ensuing discussion.

The current in the left collector of the right pair must be

$$(1-G)(Idc + Iac)$$

Continuing, the tail current in the left pair is simply Idc. Therefore, the current in the left collector of the left pair is

$$(G\ Idc)$$

The current in the right collector of that pair must be

$$(1-G)\ Idc$$

The current (I1) through the 1K resistor (R1) is

(1.6) $$I1 = G(Idc + Iac) + (1-G)Idc$$

$$= G\ Iac + Idc$$

For the differential pairs,

$$G = \frac{e^{\alpha V}}{1+e^{\alpha V}}$$

where $\alpha = kT/q$ and V is the applied bias from the outer to inner transistor bases. V is given by the sum of Vbias (<0) and the AC modulation due to the attenuated oscillator input. Since V is sufficiently negative we can write

$$1+e^{\alpha V} \doteq 1 \quad \text{and} \quad G \doteq e^{\alpha V}$$

$$G = e^{\alpha Vbias}\ e^{\alpha \nu}$$

where ν is the modulation (AC) signal. If $\nu << 1/\alpha$ (approximately 25 mV)

$$e^{\alpha N} = (1+\alpha N)$$

G now is

$$G = e^{\alpha Vbias}(1+\alpha N)$$

Putting this back into the equation 1.6,

$$I1 = e^{\alpha Vbias}(1+\alpha N)(Iac) + Idc$$

Referring to Figure 1.2 and just looking at the AC terms,

$$I1 = K1\ Ko\ Va(1+\alpha N)$$

where K1 is $e^{\alpha Vbias}$ and Ko is .857/1k. I1 now is

(1.7) $$I1 = K1\ Ko\ Va + K1\ Ko\ Va\ \alpha N$$

The PNP transistors at the top right of Figure 1.3 mirror the current to drive the crystal. They also mirror any DC component. The op-amp, resistors, transistor and capacitor of the lower right of the schematic insure that the DC level at node A is at zero volts. Should a positive DC voltage develop, the op-amp would swing positive turning the NPN transistor on more, causing more current to flow out of node A and lowering the voltage. A negative voltage would be dealt with by the transistor turning off, allowing node A to go more positive. The 10 uF capacitor is large to prevent the op-amp circuit from cancelling out the rf oscillation or modulation.

Continuing with Figure 1.3, the resistors connected to the inner bases of the 3086 are to help trim

out any non ideal characteristics as mentioned earlier.

The remaining block of Figure 1.3 is the peak detector. The same AGC circuit of Figure 1.1 is used in this circuit. The output is applied to the inner bases of the 3086 to change the overall gain.

It is important to realize the function of the quartz crystal in the circuit. A graph of the impedance and phase with respect to the input frequency of a quartz crystal is below.

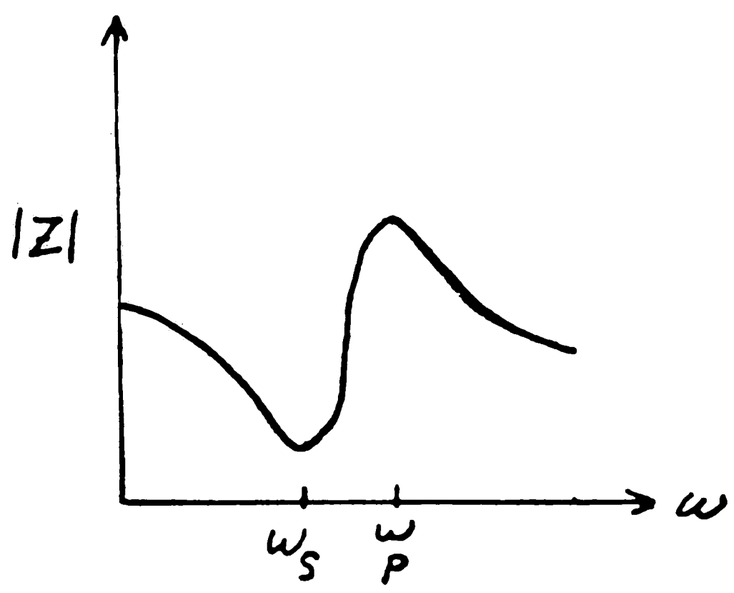

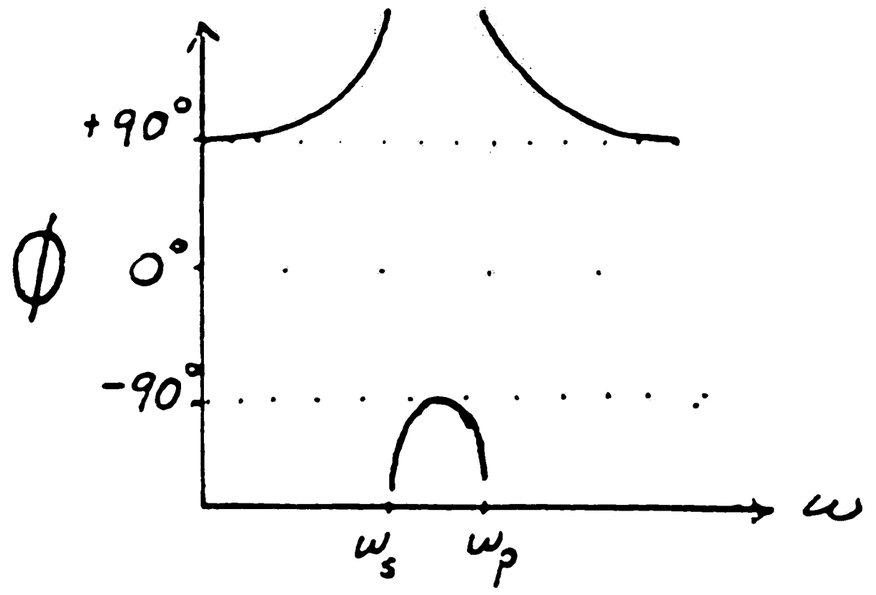

The crystal and surrounding circuitry act as a very narrow band pass filter for frequencies near parallel resonance. The sidebands (product of modulation) can just enter the passband. Any re-modulated sidebands and higher harmonics see a lower impedance and can't develop a significant voltage. As a load is applied across the crystal, the effective Q of the band pass filter becomes degraded and more sideband energy can be observed. If the amount of modulation at the crystal was observed, high resistivity loads should show little modulation. Loads of low

resistivity should show significant modulation. For the 400 KHz crystal described earlier, the impedance that the parallel resonant frequency signal sees (according to equation 1.1) is 1.1 MΩ. Sidebands 50 Hz on either side see an impedance of 990 KΩ .

Let the signal developed at the crystal be Va. As shown before,

(1.8) $$Va = I1\ Z(w)$$
$$= Ko\ K1\ (1 + \alpha\ \nu)Va\ Z(w)$$

where Z(w) is the impedance of the crystal (given by equation 1.1) at the radian frequency w. To make the math more concise, let:

$\nu = k \cos(w_m t)$ where k is the amplitude of the attenuated oscillator input and w_m is the modulating radian frequency. Also let:

$w1 = w_c + w_m$ and $w2 = w_c - w_m$ where w_c is the parallel resonant frequency (the carrier frequency).

Assume a modulated signal for the left hand side of equation 1.8 of the form,

$$Va = A \cos(w_c t) + B[\cos(w1\ t) + \cos(w2\ t)]$$
$$+ f(t)$$

where f(t) are higher order terms small enough to be

neglected (this will be verified later).

The right hand side now is

$$Va = Ko\ K1\ Z_c\ A\cos(w_c t) + Ko\ K1 \propto k \cos(w_m t) A \cos(w_c t) Z(w)$$

$$+ Ko\ K1\ B[\cos(w1\ t)+\cos(w2\ t)]\ Z(w)$$

$$+ Ko\ K1\ B[\cos(w1\ t)+\cos(w2\ t)] \propto k \cos(w_m t)\ Z(w)$$

where Z_c is the impedance at parallel resonance.

Since the amplitude of the carrier (cos w_c t) must be the

same on both sides,

$$Ko\ K1\ Z_c = 1$$

The right hand side now is

$$A\cos(w_c t) + (Z(w)/Z_c)A \propto k \cos(w_m t)\cos(w_c t)$$

$$+ (Z(w)/Z_c)B[\cos(w1\ t)+\cos(w2\ t)]$$

$$+ (Z(w)/Z_c)B \propto k[\cos(w1\ t)+\cos(w2\ t)]\cos(w_m t)$$

Multiplying and combining terms makes the right hand side

appear as

(1.9)

$$A\cos(w_c t) + (Z(w)/Z_c)\left(\frac{\propto k A}{2} + B\right)[\cos(w1\ t)+\cos(w2\ t)]$$

$$+ (Z(w)/Z_c)\frac{B \propto k}{2}[\cos(w_c t + 2w_m t)+2\cos(w_c t)$$

$$+ \cos(w_c t - 2w_m t)]$$

If we assume that $\frac{B\alpha k}{2}$ is small compared to $(\frac{\alpha k A}{2} + B)$ then looking at similar frequency terms on both sides gives

$$B = (Z(w)/Z_c)(\frac{\alpha k A}{2} + B)$$

Let

$$A' = \frac{\alpha k A}{2}$$

Solving for B we now have

$$B = \frac{A'(Z(w)/Zc}{1-(Z(w)/Zc} A \qquad (1.10)$$

A' is a constant in the circuit. $\alpha \doteq 40$, k is typically .001 v. A is determined by the AGC threshold. The constant is approximately 0.02 . B now is

$$B = \frac{0.02\ (Z(w)/Z_c)}{1-\ Z(w)/Z_c} A$$

Using $w_m = 50*2\pi$ and the impedance given earlier,

$$B = 0.18\ A$$

We can now check the validity of the assumption that f(t) was small. This is equivalent to verifying that the coefficient of the higher order term in equation 1.9 is small compared to B. In other words we must

show that

$$\frac{B \propto k}{(Z(w)/Z_c)\,|\,2} \ll \frac{k \propto A}{(Z(w)/Z_c)\,|\,2}$$

$$|\,w = w \pm 2w_m \qquad |\,w = w \pm w_m$$
$$\qquad c \qquad\qquad\qquad c$$

Due to the local symmetry of Z(w), and the fact that Z(w) is monotonically decreasing away from Z_c we get

$$Z(w_c + 2w_m) = Z(w_c - 2w_m) \quad < \quad Z(w_c + w_m) = Z(w_c - w_m)$$

Therefore we can alternately show that

$$\frac{B \propto k}{2} \ll \frac{A \propto k}{2}$$

or simply that

$$B \ll A$$

This is reasonable since for the typical case given above B = 0.18 A . Since the coefficient of the higher order harmonics is comparatively small in equation 1.9, we can conclude that f(t) can indeed be neglected, yielding the approximate form for Va given by

$$Va = A \cos(w_c t) + \frac{A'Z(w)/Zc}{1-Z(w)/Zc} A\,[\cos(w_1 t)+\cos(w_2 t)]$$

where $Z(w)=Z(w_1)=Z(w_2)$

Finally, it is necessary to show how the amount of modulation is related to the effective Q of the

crystal. For simplicity, a quartz crystal near parallel resonance can be modeled as a parallel RLC circuit with R being the effective parallel resonance resistance and L and C being the equivalent parallel inductance and capacitance. The impedance of the equivalent model is

$$Z(w) = \frac{jwL}{-w^2 CL + jw\frac{L}{R} + 1}$$

$$= R*H(w)$$

where

$$H(w) = \frac{j\frac{w}{w_o Q}}{1 - \frac{w^2}{w_o^2} + j\frac{w}{w_o Q}}$$

where $w_o = \frac{1}{\sqrt{LC}}$ and $Q = R\sqrt{\frac{C}{L}}$

Note that when $w=w_o$, $H(w)=1$ and $Z_c = R$. Therefore $Z(w)/Z_c = H(w)$.

The magnitude of H(w) is

$$|H(w)| = \frac{\frac{w}{w_o Q}}{\sqrt{\left(1-\left(\frac{w}{w_o}\right)^2\right)^2 + \left(\frac{w}{w_o Q}\right)^2}}$$

If we let $w = w_o + w_m$ and let $w_m / w_o = d$, then some algebra can show

$$|H(w)| = \frac{1}{\sqrt{1+4d^2Q^2}}$$

Assuming that since $4d^2Q^2 << 1$, then using the first two terms of the binomial expansion it can be shown that,

$$|H(w)| = \frac{1}{1+2d^2Q^2}$$

This approximation is valid considering the values given earlier.

Remembering that $Z(w) = R*H(w)$ and looking at equation 1.10 we find that the amplitude of the sidebands is given by

$$B = \frac{A'H(w)}{1 - H(w)} A$$

Substituting the above result yields

$$B = \frac{A'}{2\,d\,Q^2}\,A^2$$

This makes the amount of sideband energy inversely proportional to Q^2. Keeping in mind that Q is proportional to R, and B is inversely proportional to R^2, as the effective resistance of the parallel RLC model is decreased, Q is decreased and the amplitude of sidebands increases.

There are two approaches to using the crystal oscillator described. The amount of modulation observed at the crystal can be expected to increase as the load resistor decreases, or the DC level of the AGC (Vbias) can be expected to increase as the resistance of the load decreases. The DC level was recorded for the experiment below. Further on, a different modulation scheme is used and the AC signal is observed.

Using the Oscillator

As discussed in Chapter 3, the model for a semiconductor on a capacitance probe can be a series RC network with the R being the effective resistance through the semiconductor. For this reason, series combinations of resistors and capacitors were placed across the crystal and the DC output of the AGC was monitored. The crystal frequency was 315830 Hz. and the modulation frequency was 50 Hz. A graphical representation of this experiment is Figure

1.5. This method seems to have potential for testing effective resistances from 100Ω to 8KΩ or from 50KΩto 800KΩ. Unfortunately, it is not obvious how to discriminate between the two ranges. When silicon wafers were placed on a probe made of two half-circles on an etched PC board, the result is Figure 1.6. Again, the dip in the center of the resistivity range makes this method difficult to implement for silicon.

Some problems encountered include somewhat erratic frequency shifts for different crystal loadings. It seems reasonable that the added capacitance can change the crystal frequency, and frequency shifts of 100 Hz. were common. The added capacitance along with the proximity of the crystal's parallel mode to its series mode help to explain the unstable frequencies. The lower sideband may see some effects of the lower impedance and phase shifts of the series mode. Circuit modifications including changing the time constant of the AGC, changing the crystal and changing the probe geometries did not significantly change the data presented.

Chopping a Load Across the Crystal

A different approach to the modulation method was to ground the modulation input of Figure 1.3 and modulate the signal at the crystal by switching between a series RC to ground and just a capacitor to ground.

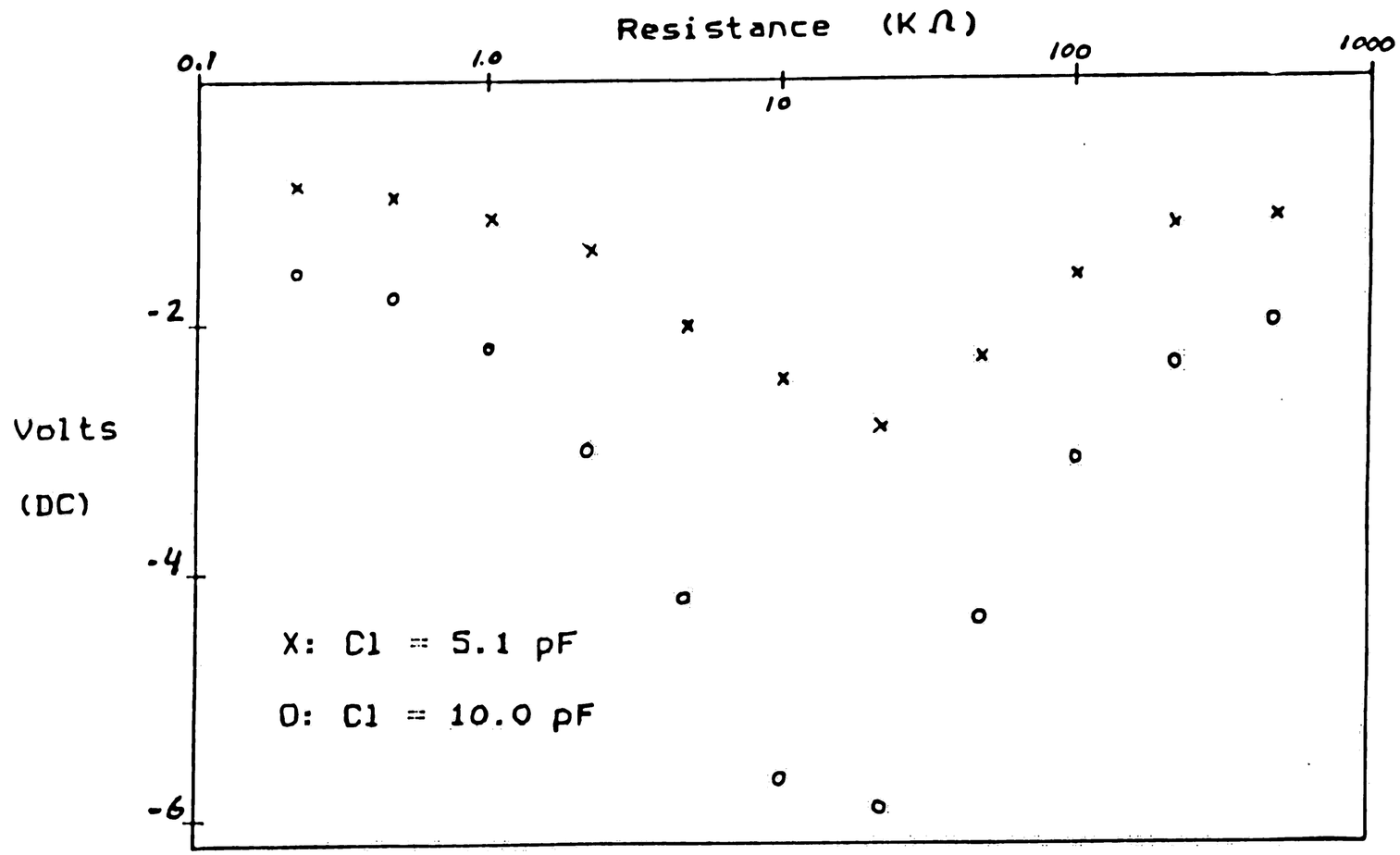

Figure 1.5 Graph of DC Voltage out of AGC for Resistors Soldered across Crystal

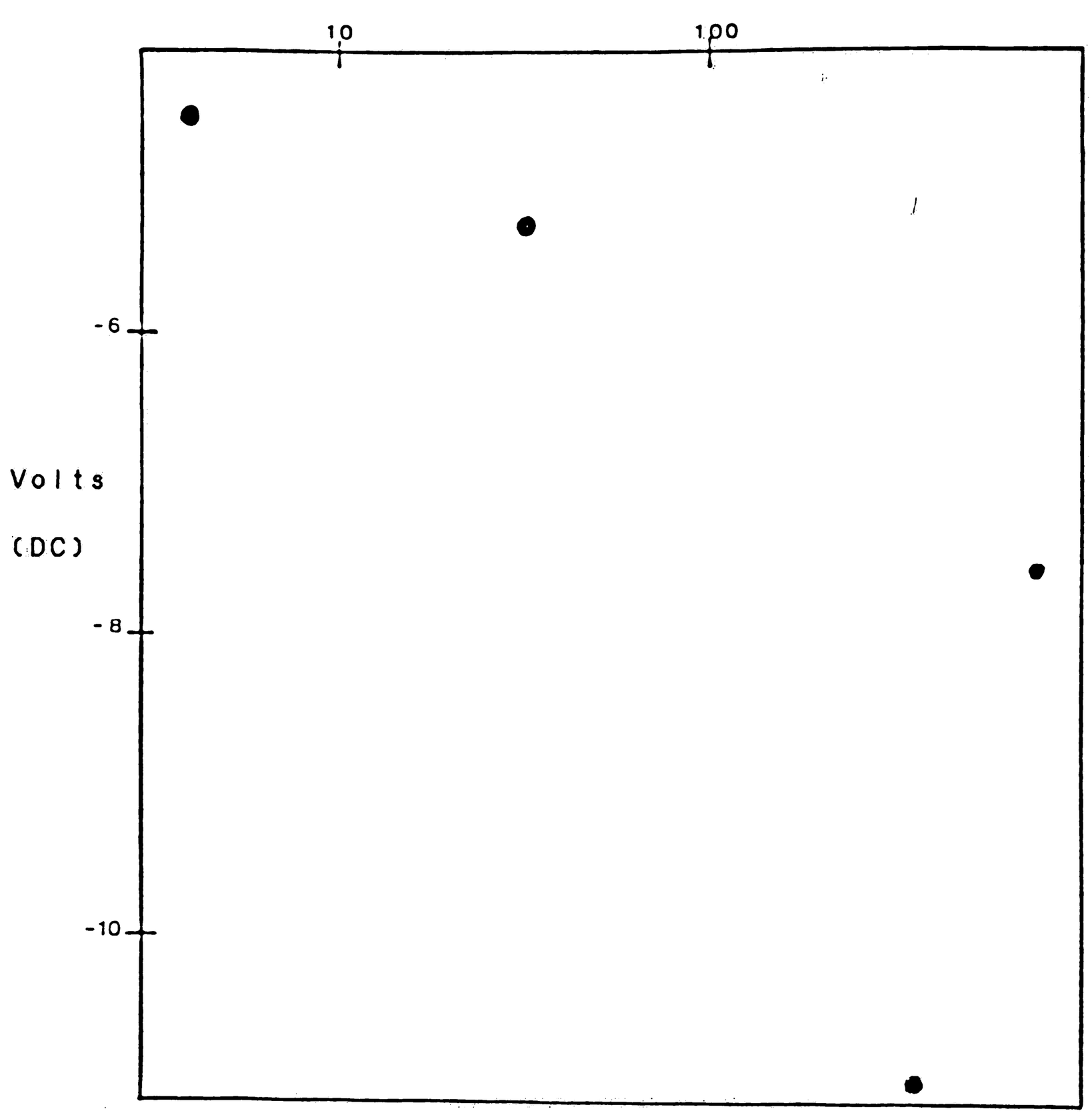

Figure 1.6 Graph of DC Output for Silicon Samples on Probe in Parallel with Quartz Crystal

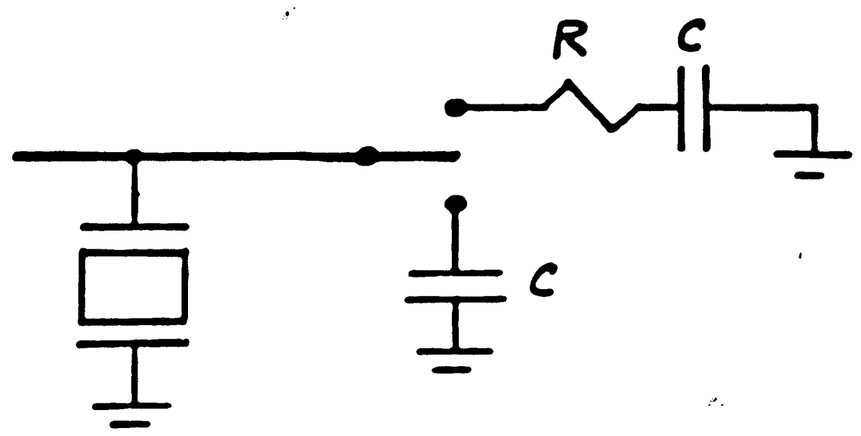

A graph of the AC out of the AGC for different resistors and switching frequencies is figure 1.7. A slower switching frequency seems to cause a greater range in the output voltage, but the graph shows a nonlinear trend. As with the first method, it would be impossible to tell which side of the peak an unknown would be on. A fast switching speed tends to make the graph more linear at the cost of smaller differences in output between samples. Figure 1.8 shows the result of the resistor replaced by the probe loaded with silicon wafers and different values of C. 10 pF offered the greatest change in output voltage for the samples, but the lower resistivities could not be resolved.

The three methods discussed above showed limited success as resistivity determining systems. A major difficulty is finding a way to remove enough energy from a resonant circuit to detect it without changing the resonant frequency. It is not apparent that this can be done when a capacitive probe is used in parallel with a quartz crystal.

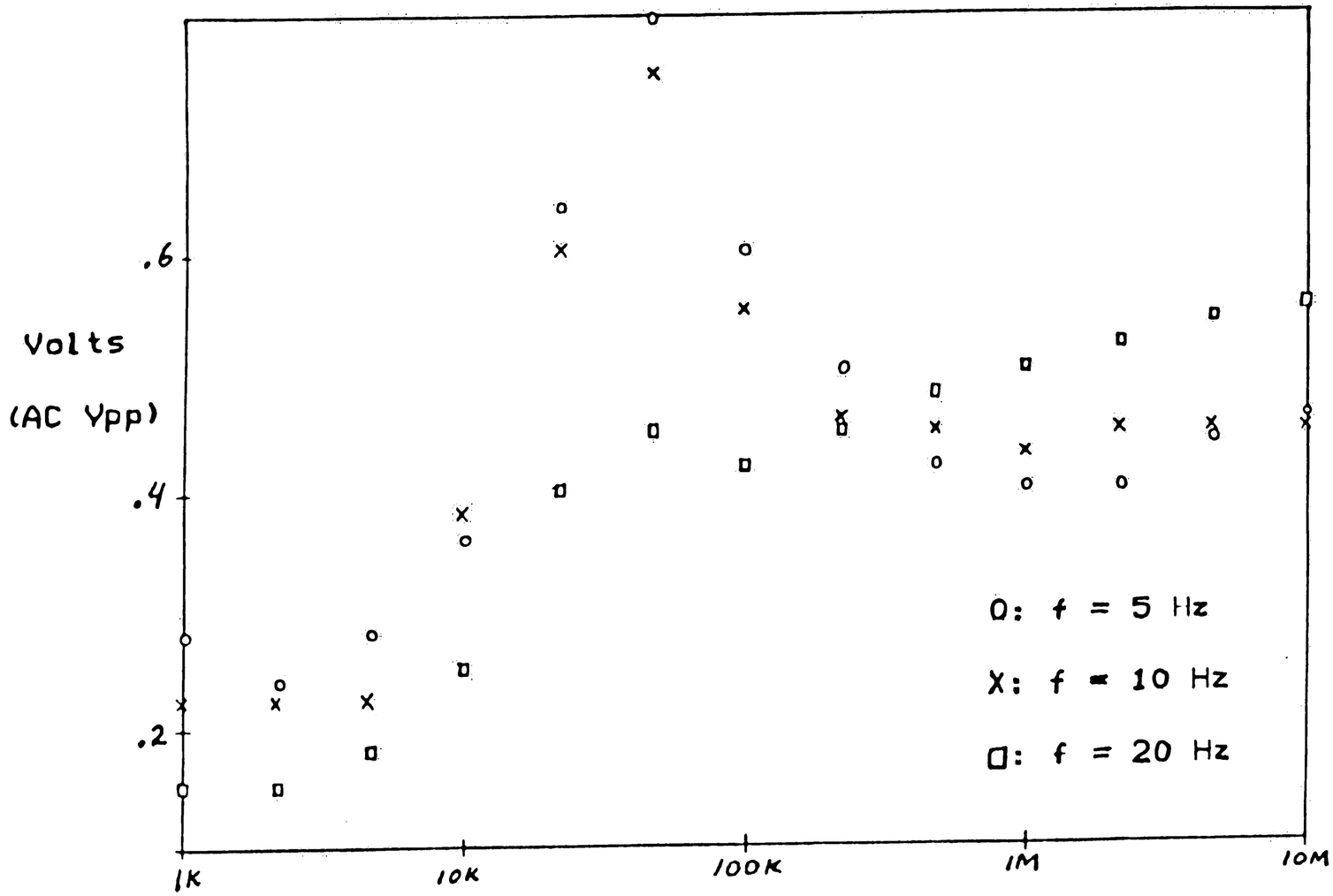

Figure 1.7 Graph of AC Output of AGC for Resistors Soldered across Quartz Crystal for Different Modulating Frequencies

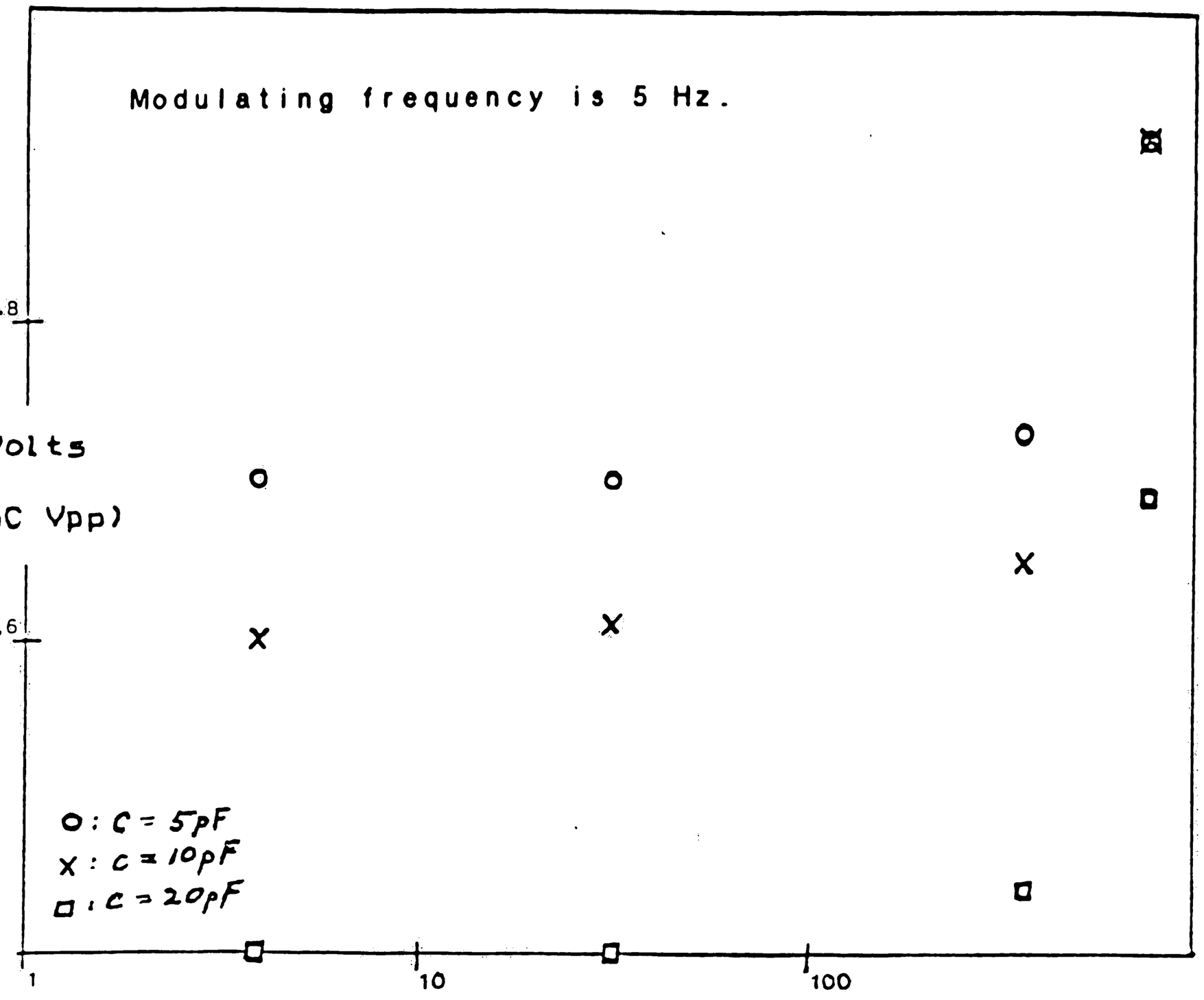

Figure 1.8 Graph of AC Output for Silicon Samples on Probe

It seems a system that can make the capacitance of the loaded probe and the operating frequency constant for any loading, or one that can take into account the change in frequency in accordance with the above equations seems necessary. Systems like that were not investigated.

CHAPTER TWO

Resistivity Measurement by Quadrature Detection

A completely different method to determine the resistivity of a semiconductor is Quadrature Detection. This method relies on a model for a semiconductor on a capacitance probe, a summing amplifier, a multiplier and low pass filters.

The model used to describe a semiconductor on a capacitance probe is a series RC model with C_s as the coupling capacitance and R_s as the resistance through the semiconductor.

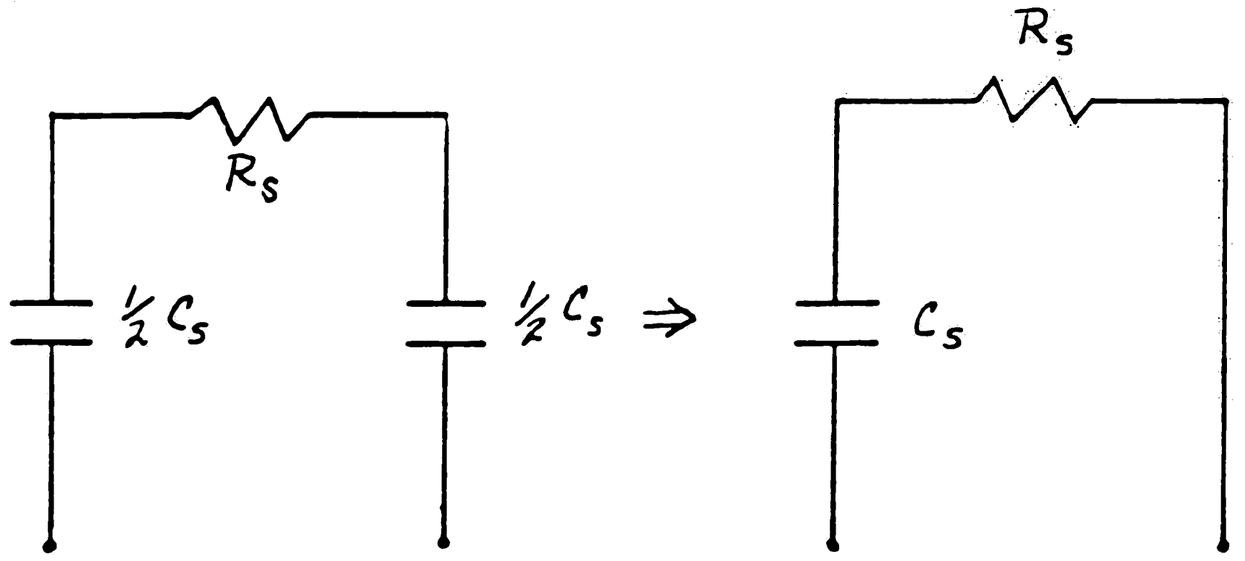

In Chapter 3 it is shown how a series RC can be modeled as a parallel RC combination

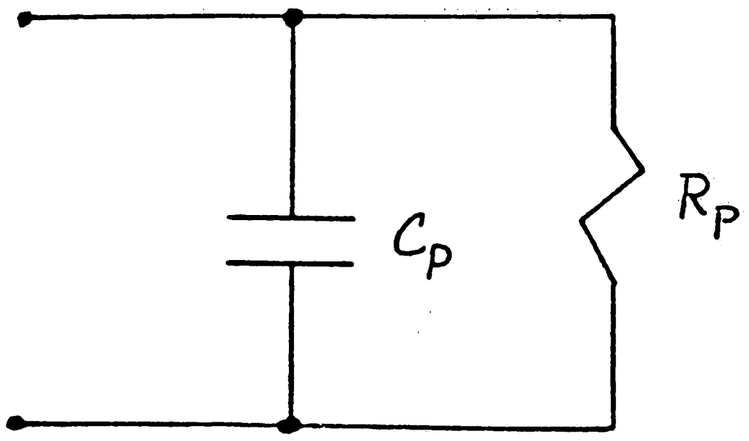

as long as the equation relating the impedance of both models is satisfied, namely,

$$Rs - j\frac{1}{wCs} = \frac{Rp}{1+w^2 Cp^2 Rp^2} - j\frac{w Rp^2 Cp}{1+w^2 Cp^2 Rp^2}$$

If a parallel RC is used as the input to a summing amplifier, the output would consist of two componants; one in phase with the input due to the resistor and one 90 degrees out of phase due to the capacitor.

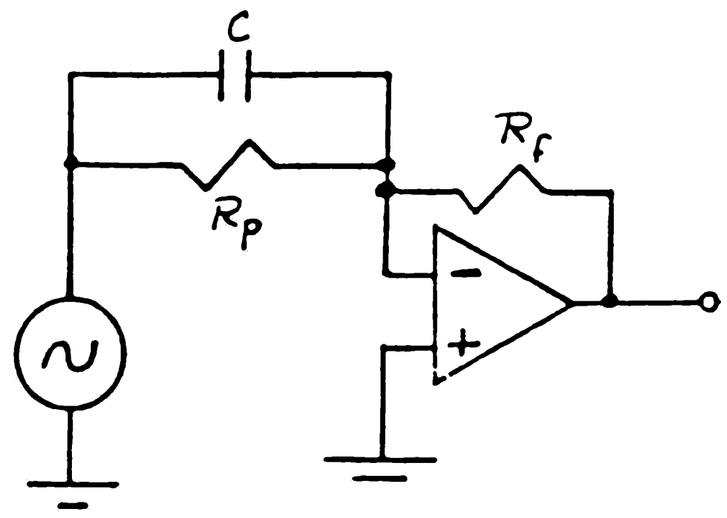

More specifically,

$$Vo = -Rf/Rp\ Vin + j\ Rf\ w\ C\ Vin$$

$$= A\ Vin + j\ B\ Vin$$

$$= A\ \cos(wt) + j\ B\ \cos(wt)$$

$$= A\ \cos(wt) + B\ \sin(wt)$$

If this signal is multiplied by a signal in phase with the real componant (cos wt), the result would be

$$Vo = [\cos(wt)]*[A\ \cos(wt) + B\ \sin(wt)]$$

$$= A \cos^2(wt) + B \sin(wt) \cos(wt)$$

$$= A/2\,[\cos(0)+\cos(2wt)] + B/2\,[\sin(0)+\sin(2wt)]$$

$$= A/2 + A/2 \cos(2wt) + B/2 \sin(2wt)$$

If Vo was passed through a low pass filter with the cutoff approaching DC, the output would be directly proportional to Rf/Rp. Since Rp is of interest, the output is inversly proportional to the resistance.

Figure 2.1 shows a system diagram of a circuit to perform the above function. Figure 2.2 is the actual circuit. Appendix I and Appendix II discuss the phase shifters and low pass filters in some detail. The phase shifters are used to compensate for non-ideal elements used. With no Rp in place (Rp=∞, Rs=0), the DC output (hereafter refered to as simply output) should be zero volts. The phase shifters were used to achieve this. Various sized resistors were used as Rp and the output recorded. Figure 2.3 shows the results of this experiment.

Next, a probe was made by drawing two half circles on a piece of PC board and etching away the unprotected copper. The probe replaced the Rp and Cp in the above circuits, and the phase was adjusted to give zero DC out when no sample was on the probe. When samples of GaAs were placed across the gap in the probe, the output drifted severly and was very sensitive to our position. Attempts to

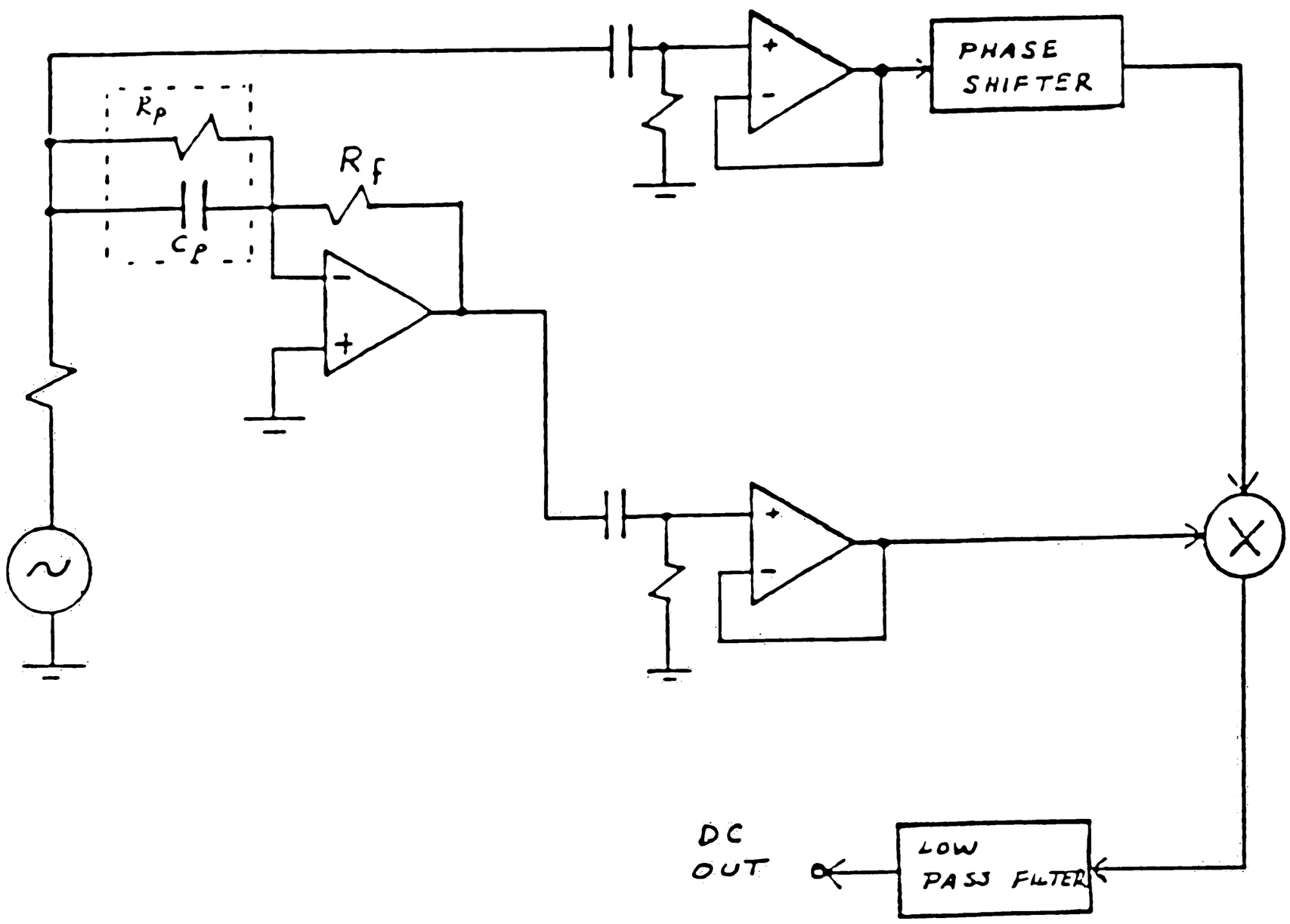

Figure 2.1 System Diagram of Resistivity Measuring Circuit using Quadrature Detection

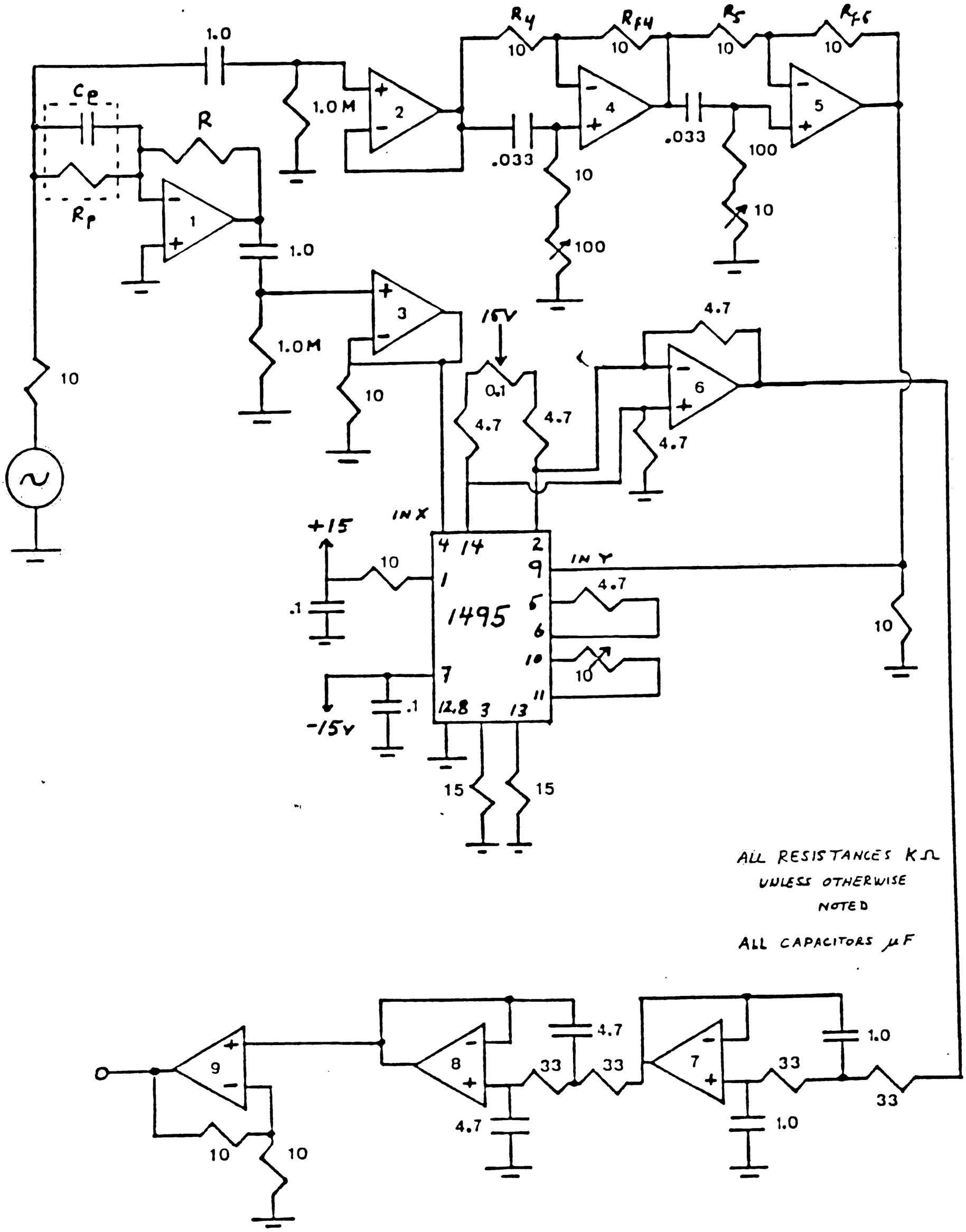

ALL RESISTANCES KΩ
UNLESS OTHERWISE
NOTED

ALL CAPACITORS μF

Figure 2.2 Schematic of Circuit to Measure Resistivity by Quadrature Detection

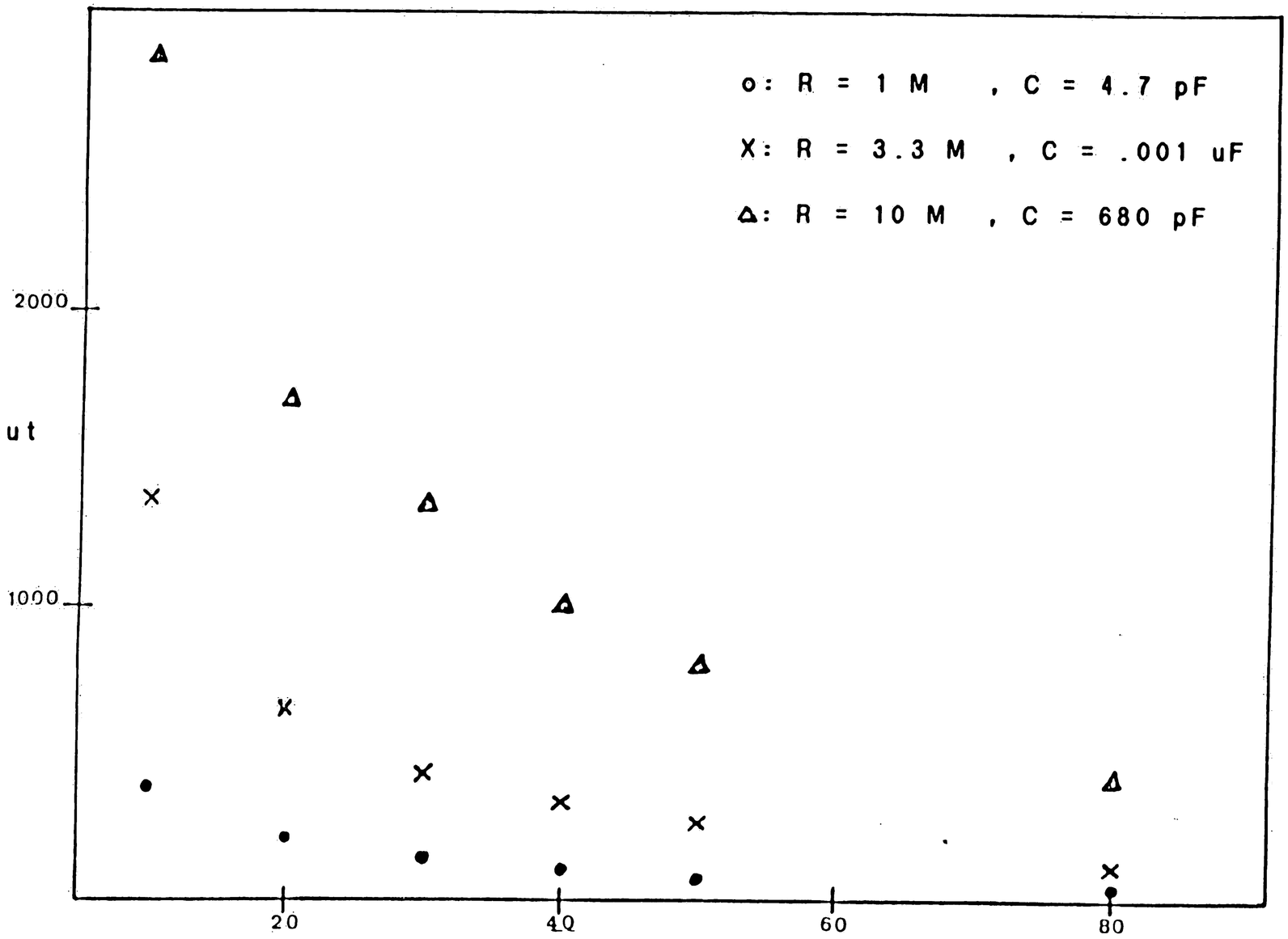

Figure 2.3 Graph of DC Output for Various Sized Resistors

shield the probe and multiplier with metal boxes and foil did not help. It was impossible to get any consistant reading for GaAs samples in the 10^7 to 10^9 ohm cm. range. One reason for the difficulty is that the op-amps used were non-ideal; the DC output due to input bias currents and input offset voltages could overwhelm the DC output that is inversly proportional to the resistivity of the samples.

A discussion of the magnitude of the offsets is as follows. Any DC offset from the reference signal would be blocked by the capacitor before entering OA2. (see Figure 2.1). However, OA2 adds its own offset (V2) to the signal. Refering to Figure 2.2 , there is a DC path to the multiplier from OA2. To DC, the phase shifters look like inverting amplifiers. The DC output of OA4 is

$$(V2 * Rf4/R4) + V4$$

In the same manner, the DC output of OA5 is

$$[(V2 * Rf4/R4) + V4] * Rf5/R5$$

The y input to the multiplier now is

$$([(V2 * Rf4/R4) + V4] * Rf5/R5) + V5 + \cos(wt)$$

Similarly, the total x input to the multiplier is

$$A \cos(wt) + B \sin(wt) + V3$$

After multiplication (and neglecting any multiplier errors) the DC componant before entering the low pass filters is

$$V2\ V3 + \frac{Rf4\ Rf5}{R4\ R5} + V3\ V4\ \frac{Rf5}{R5} + V3\ V5 + V6 + A/2$$

The first two op-amps (#7 and #8) look like voltage followers to the DC signal. Again each adds its own offset. The final op-amp looks like a non-inverting amplifier with gain of two (1 + Rf9/R9 = 2). Since offsets are on the order of millivolts, the significant output terms are

$$Vo = 2 * (V6 + V7 + V8 + V9) + A$$

Recalling that A is inversly proportional to the resistivity and that the resistivity of GaAs is very high, it seems reasonable to expect that A may not dominate the output. If we assume 5 mV of offset (reasonable for the op-amps used) the error term could be as large as 40 mV. For very low resistivities this may not be significant (the desired output term should be large) but for resistivities approaching the range of GaAs, 40 mV is devistating. Since the resistance through the sample is a function of the length of the path through that sample, probes with closer spacing may reduce the effective resistance so that the A term may dominate for higher resistivity samples.

In attempts to reduce noise, the quadrature circuit was redesigned so that the load (probe) was measured differentially. Attenuators were added to make the inputs to the multiplier of the same amplitude. Figure 2.4 shows the circuit. As a test, parallel RC combinations were soldered in place. The results were encouraging enough

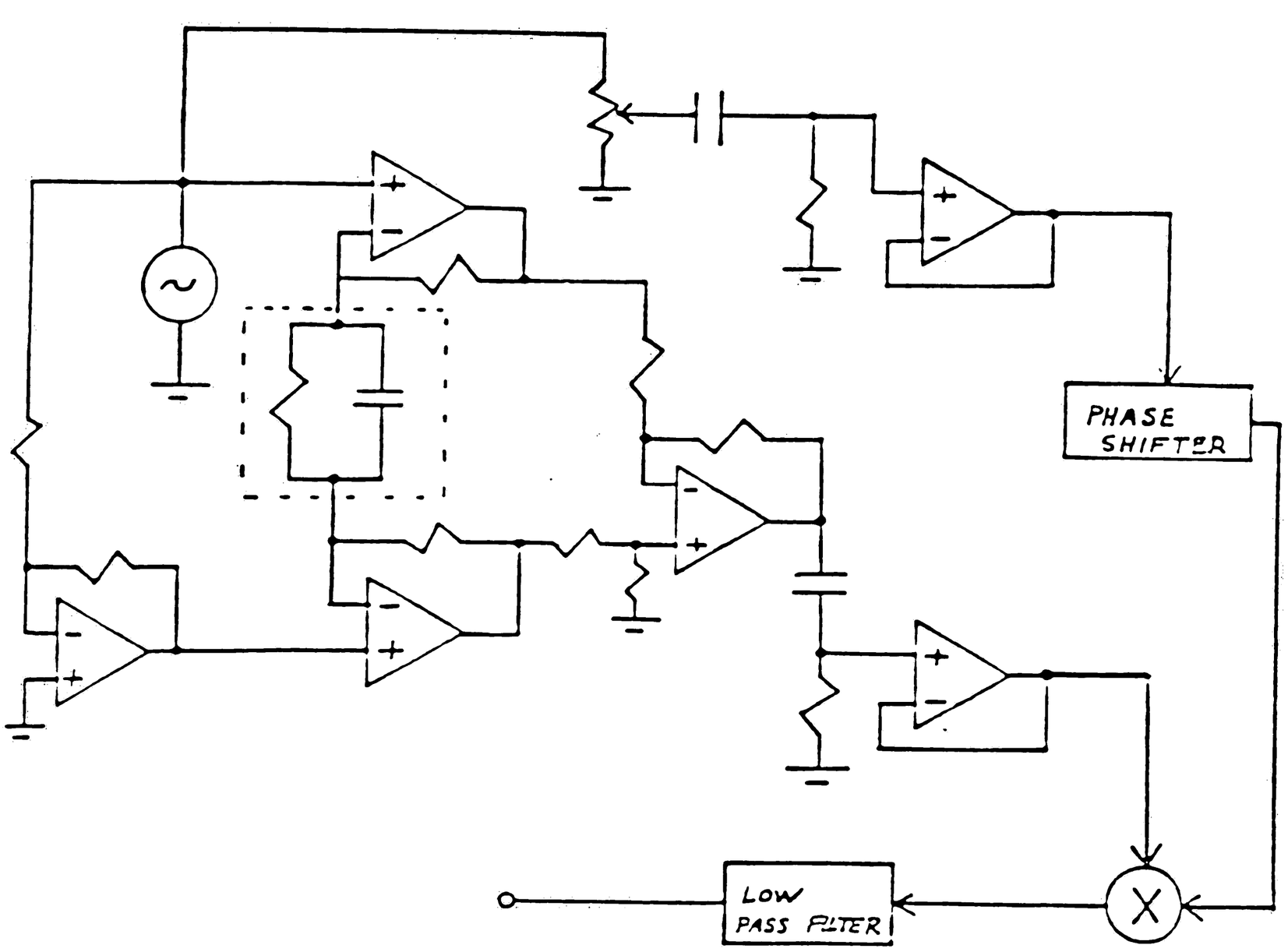

Figure 2.4 Diagram of Quadrature Circuit to Determine Resistivity Differentially

to try the probe again (see Figure 2.5). Drifting was still a problem. Changing the input frequency offered no added stability.

In a final attempt to reduce drifting problems and make the circuit less sensitive to our presence, the probe was switched in and out of the circuit by relays operated from a remote location. The probe was switched in (unloaded), and DC readings were taken. Then the probe was switched out and loaded, switched back in and the DC was recorded. Next the probe was probe switched out and unloaded. Finally the probe was switched back in and DC recorded. The average change in the DC value for the loaded and unloaded probe as a function of the resistivity is Figure 2.6 . Unfortunately, the same circuits that contributed to the error of the first method (the phase shifters, multiplier and low pass filter) were also used in the differential method.

Attempts at looking at GaAs by quadrature detection were not entirely successful with the circuits used. Noise was a big concern. Figure 2.5 shows the output for different resistors up to 100 MΩ. At this point the output was fluctuating by as much as 30 mV. It seems certain that the output for resistances approaching that of GaAs would be totally lost in the inherant noise.

Quieter and better shielded circuits could improve

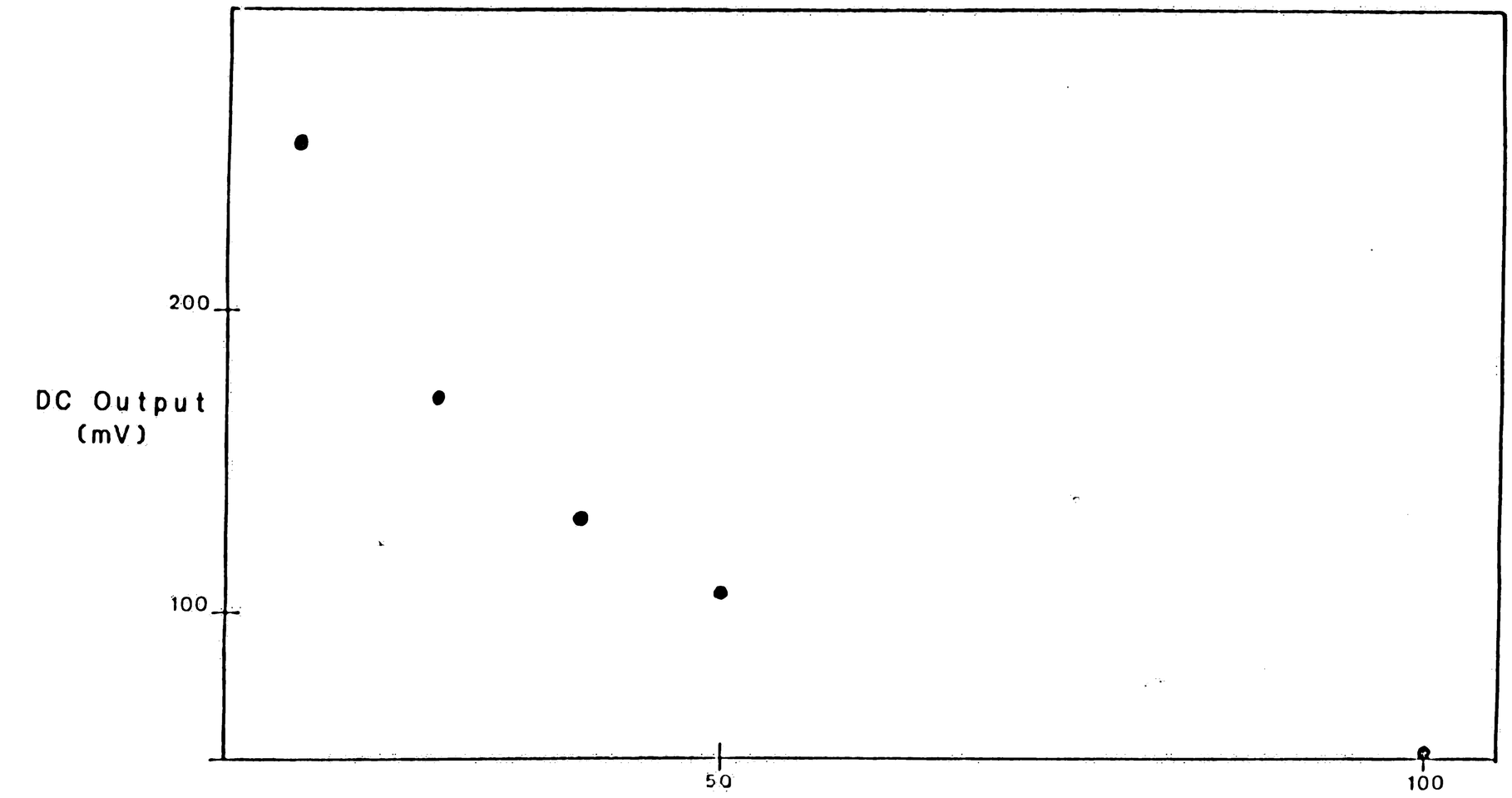

Figure 2.5 Graph of DC Output for Resistors Measured Differentially

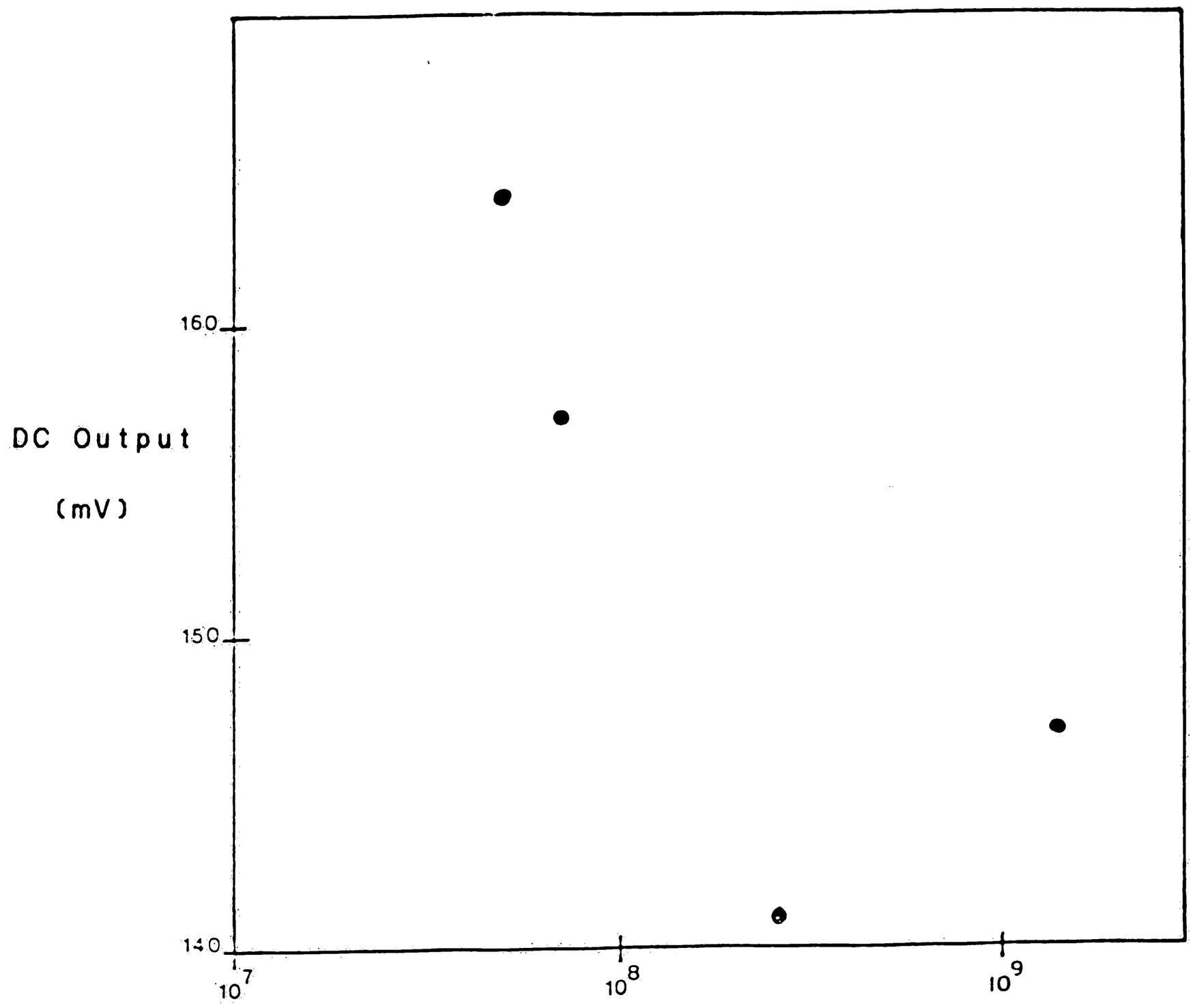

Figure 2.6 Graph of DC Output vs Resistivity for Silicon Sampled Measured Differentially

results. As was discovered later, probe surfaces smaller than the samples did give better results (see Chapter 3). The final method looked at for determining resistivity involves a HP LCR Meter (model 4261 A) that uses quadrature detection with more sophisticated circuitry than presented here.

CHAPTER THREE

Resistivity Measurement Using an LCR Meter

The final measurement technique involves placing a sample of GaAs on a probe made of an etched PC board. The loaded probe is connected to an LCR meter (Hewlett-Packard model 4261 A) and the readings of capacitance and dissipation are recorded. Ideally, some mathematics could transform samples of known resistivity to a line on a graph. Unknowns would find their place on the line and the resistivity read off the axis.

Model for GaAs on Capacitance Probe

The original model for a sample of GaAs on a probe was a series RC model,

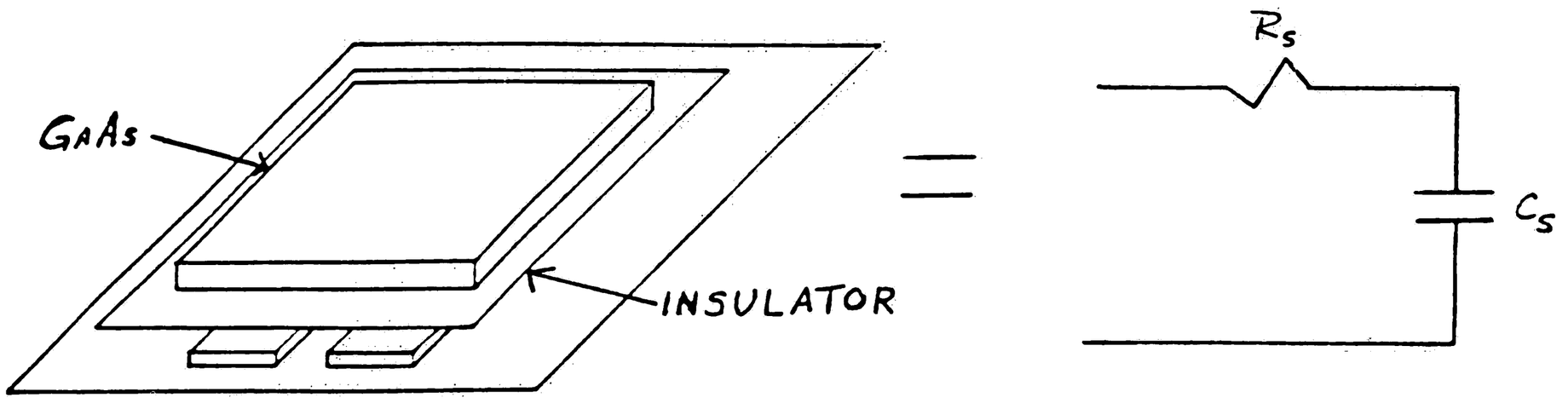

where Cs is the coupling capacitance between the probe and sample and Rs is the resistance through the crystal. When the loaded probe is connected to the LCR meter, the meter gives readings for the parallel mode.

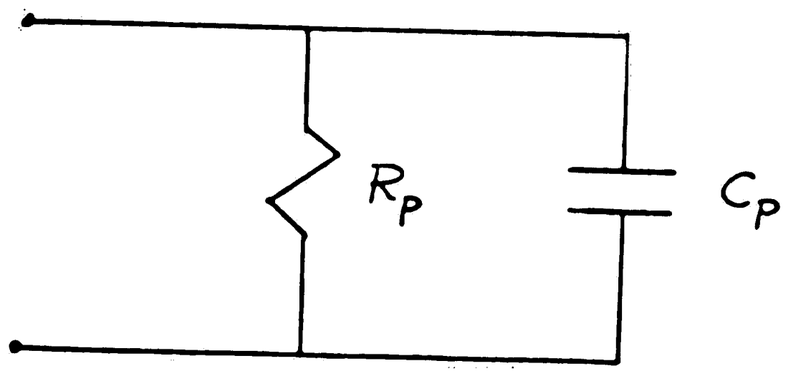

It is therefore necessary to equate the two models.

The impedance of the series model is

$$Zs = Rs - j\ 1/(wCs)$$

The parallel impedance is

$$Zp = \frac{Rp}{1+w^2 Cp^2 Rp^2} - j\frac{w^2 Rp^2 Cp}{1+w^2 Cp^2 Rp^2}$$

For the parallel model to be equivalent to the series model, the magnitudes of the real and imaginary parts must be equal. Hence, we require that

$$Rs = \frac{Rp}{1+w^2 Cp^2 Rp^2}$$

$$\frac{1}{wCs} = \frac{w^2 Rp^2 Cp}{1+w^2 Cp^2 Rp^2}$$

If the real and imaginary parts are equal, then the angle between them must also be equal. Specifically,

$$\text{Tan}^{-1}\frac{1}{w\,Cs\,Rs} = \text{Tan}^{-1}\frac{w\,Rp^{2}\,Cp}{Rp}$$

Therefore,

$$\frac{1}{w\,Rs\,Cs} = w\,Rp\,Cp$$

The value of dissipation (D) given by the LCR meter is defined as

$$D = w\,Cs\,Rs = \frac{1}{w\,Cp\,Rp}$$

and is 1/Q of the models.

Setting the real parts equal to each other now gives

$$Rs = \frac{Rp}{1+w^{2}\,Cp^{2}\,Rp^{2}}$$

Using

$$D = \frac{1}{w\,Cp\,Rp}$$

$$Rs = \frac{Rp}{1+1/D^{2}}$$

$$Rs = \frac{D^{2}}{D^{2}+1}\,Rp$$

Pursuing the real part further,

$$R_p^2 (\omega^2 C_p^2 R_s^2) - R_p^2 + R_s^2 = 0$$

Using the quadratic formula,

$$R_p = \frac{1 \pm \sqrt{1 - 4\omega^2 C_p^2 R_s^2}}{2\omega^2 C_p^2 R_p}$$

Since Rp is real,

$$4\omega^2 C_p^2 R_s^2 < 1$$

$$2\omega C_p R_s < 1$$

$$R_s < \frac{1}{2\omega C_p}$$

The reactive parts must also be equal.

$$\frac{1}{\omega C_s} = \frac{\omega^2 R_p^2 C_p}{1 + \omega^2 C_p^2 R_p^2}$$

$$C_s = \frac{1 + 1/D^2}{1/D^2} C_p$$

$$C_s = (D^2 + 1) C_p$$

Continuing with the imaginary parts,

$$Cp^2 (Rp^2 w^2) - Cp^2 (Rp^2 w^2 Cs) + 1 = 0$$

$$Cp = \frac{Rp^2 w^2 Cs \pm \sqrt{Rp^4 w^4 Cs^2 - 4Rp^2 w^2}}{2Rp^2 w^2}$$

Since Rp is real,

$$Rp^4 w^4 Cs^2 > 4Rp^2 w^2$$

$$Rp^2 w^2 Cs^2 > 2 Rp^2 w^2$$

$$Cs > \frac{2}{Rp^2 w^2}$$

Now both models are related by

$$Rs = \frac{D^2}{D^2 + 1} Rp$$

$$Cs = (D^2 + 1) Cp$$

where

$$D = w Cs Rs = \frac{1}{w Cp Rp}$$

and the relationships

$$Rs < \frac{1}{2 w Cp}$$

$$Cs > \frac{2}{Rp\ w}$$

must be met.

Experiment

In a typical experiment, samples are placed on top of a probe connected to the LCR meter (discussion of the probe follows). The meter is set up as follows:

f=1kHz

Bias=1.5v

Signal=1v

AUTO or PARA mode

After a minimum of 60 minutes warm up, samples of GaAs are introduced to the probe and readings of dissipation and capacitance are recorded. Rp is calculated by

$$Rp = \frac{1}{2\pi\ w\ Cp\ D}$$

A typical graph is Figure 3.1a .

Correction for Rp

The shape of the data suggested a different model for the crystal on the probe:

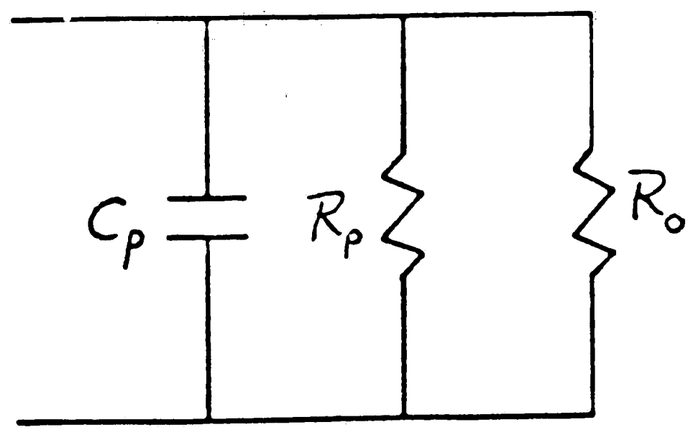

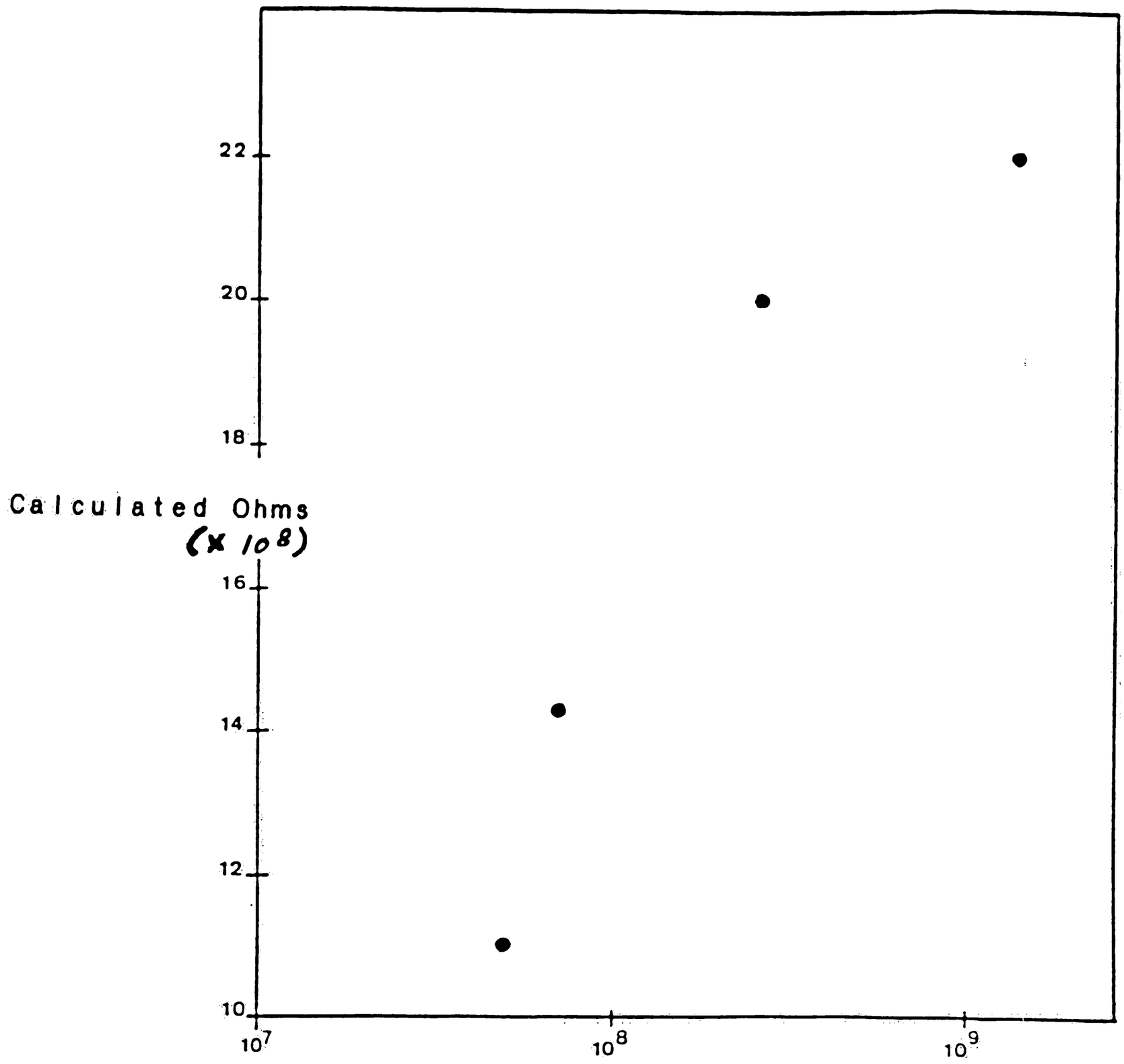

Figure 3.1a Graph of Calculated Rp as a Function of Known Resistivity For GaAs Samples

where Ro is constant and is a function of the probe, wires and input impedance of the meter. Now the Rp derived from the C and D is actually Rpeq and

$$Rpeq = Rp\ Ro/(Rp+Ro)$$

So now,

$$Rp = Ro\ Rpeq/(Ro-Rpeq)$$

The derivation of Ro is given in Appendix III.

Observations gave another method to determine Ro. When the probe is unloaded, there are values for C and D given. Since the probe is unloaded, the Rp calculated is simply Ro. Both methods for calculating Ro agree to within 5%. The data with the Ro correction is Figure 3.1b .

Correction for Cp and D

Since a capacitance value is given for the unloaded probe, there must be a standing capacitance Co, and that can be read directly from the meter. The model for a semiconductor on the probe now is

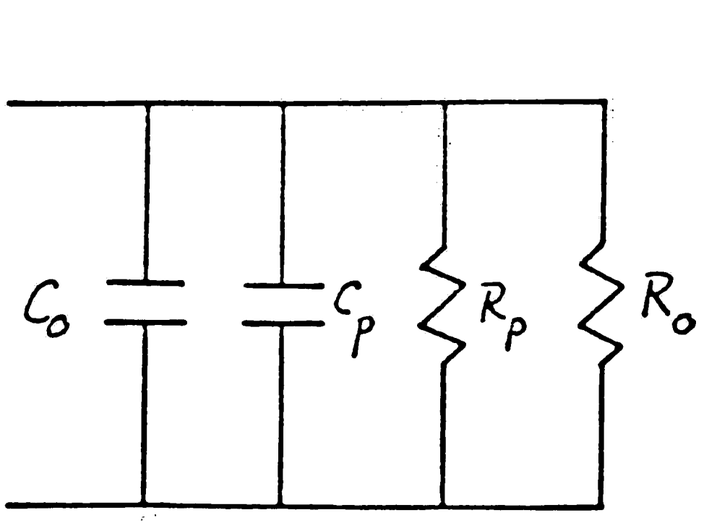

which transforms to

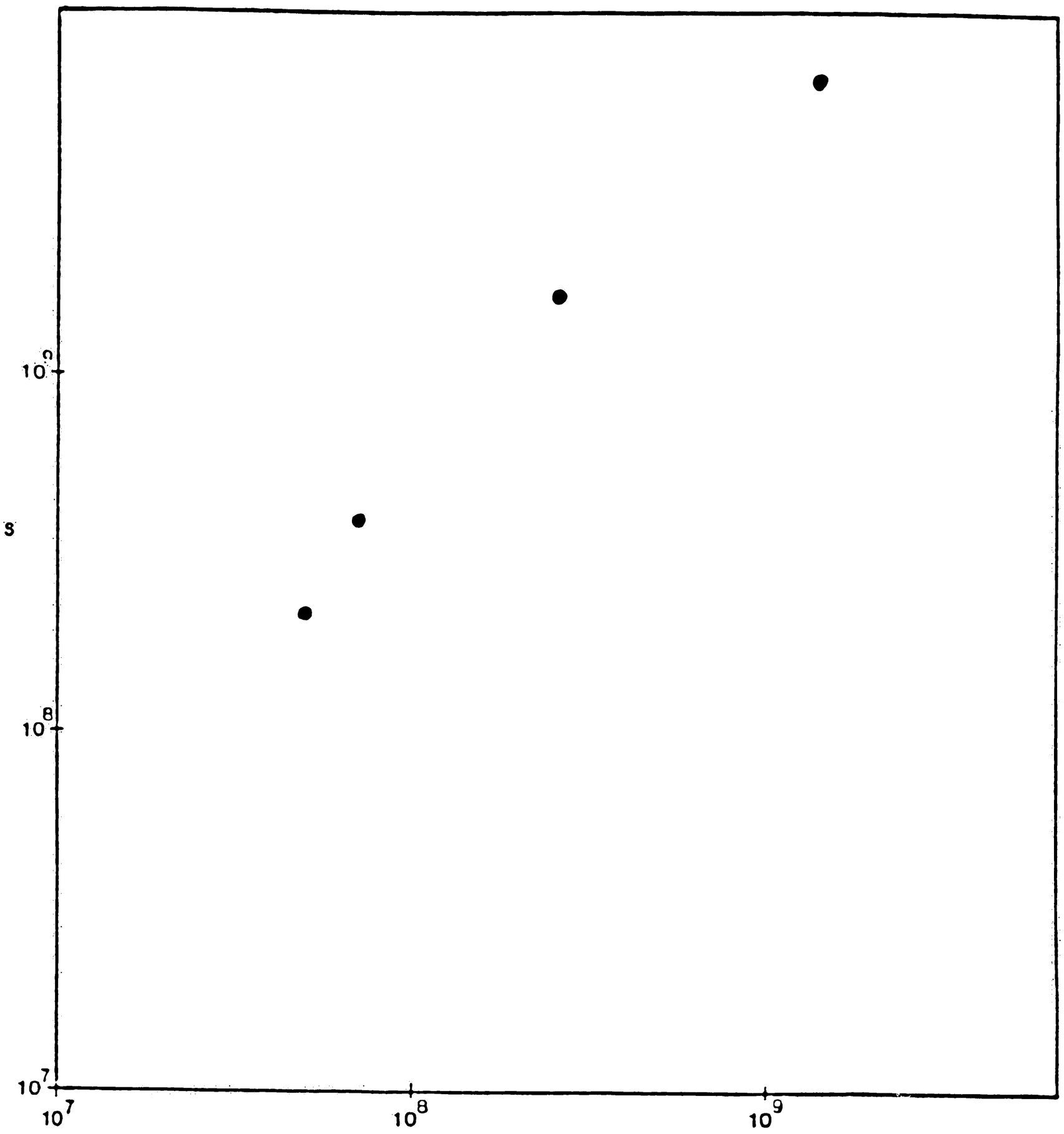

Figure 3.1b Graph of Rp vs Resistivity with Ro Correction

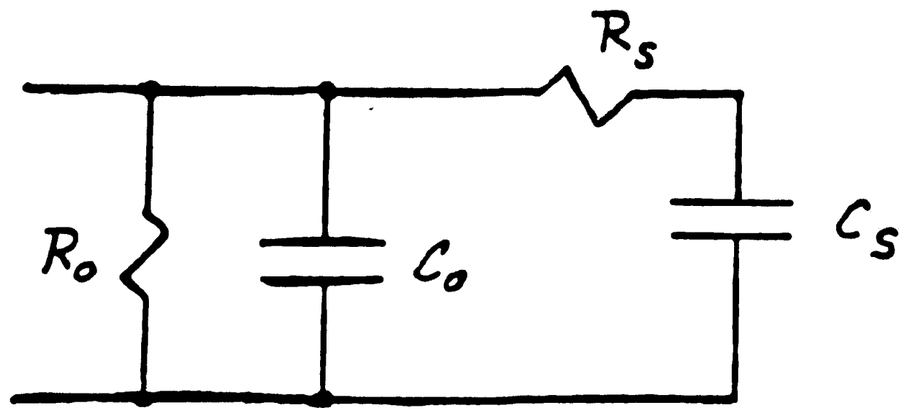

The D reading given by the meter is now

actually

$$D_{eq} = \frac{1}{w\ C_{eq}\ R_{peq}}$$

where

$$C_{eq} = C_o + C_p$$

and

$$R_{peq} = \frac{R_p\ R_o}{R_p + R_o}$$

If the relationship

$$R_s = \frac{D^2}{1 + D^2} R_p$$

is to be used to find Rs, a new value for D must be calculated that removes the effects of Co and Ro. The D that we are interested in is

$$D = \frac{1}{C_p\ R_p\ w}$$

so the following calculation must be performed

$$D = \frac{R_o}{R_p + R_o} \frac{C_{eq}}{C_p} D_{eq}$$

Results of Corrections

To reiterate, Ro and Co are found from the unloaded probe. The difference in capacitance between the loaded and unloaded probe is Cp. Rp is calculated from Ro, and Ceq and Rpeq as read from the meter. These values are used to establish a new D that transforms Rp data into Rs data. Figure 3.2 shows a graph of Rp and Rs. Note that more samples were added.

For the final experiment, more samples were added. Figure 3.3 shows this result. The data for Rp has the general shape and orientation that was hoped for, but only if the points are fitted to a straight line. This data is promising all the way up to the 10 ohm cm. range, but the points are all not close enough to the line to make any accurate resistivity measurement. The Rs data shows the now characteristic dip at the high resistivity end. This roll off around $5*10^{8}$ ohm cm. is not understood. For resistivities from $2*10^{7}$ to $5*10^{8}$ the Rs data appears as good as the Rp data (but still not good enough to give accurate results with an unknown).

A straight line at 45 degrees was expected. The values for capacitance are in the 10 pF range. Moving the probe relative to the meter can cause as much as 1.2 pF

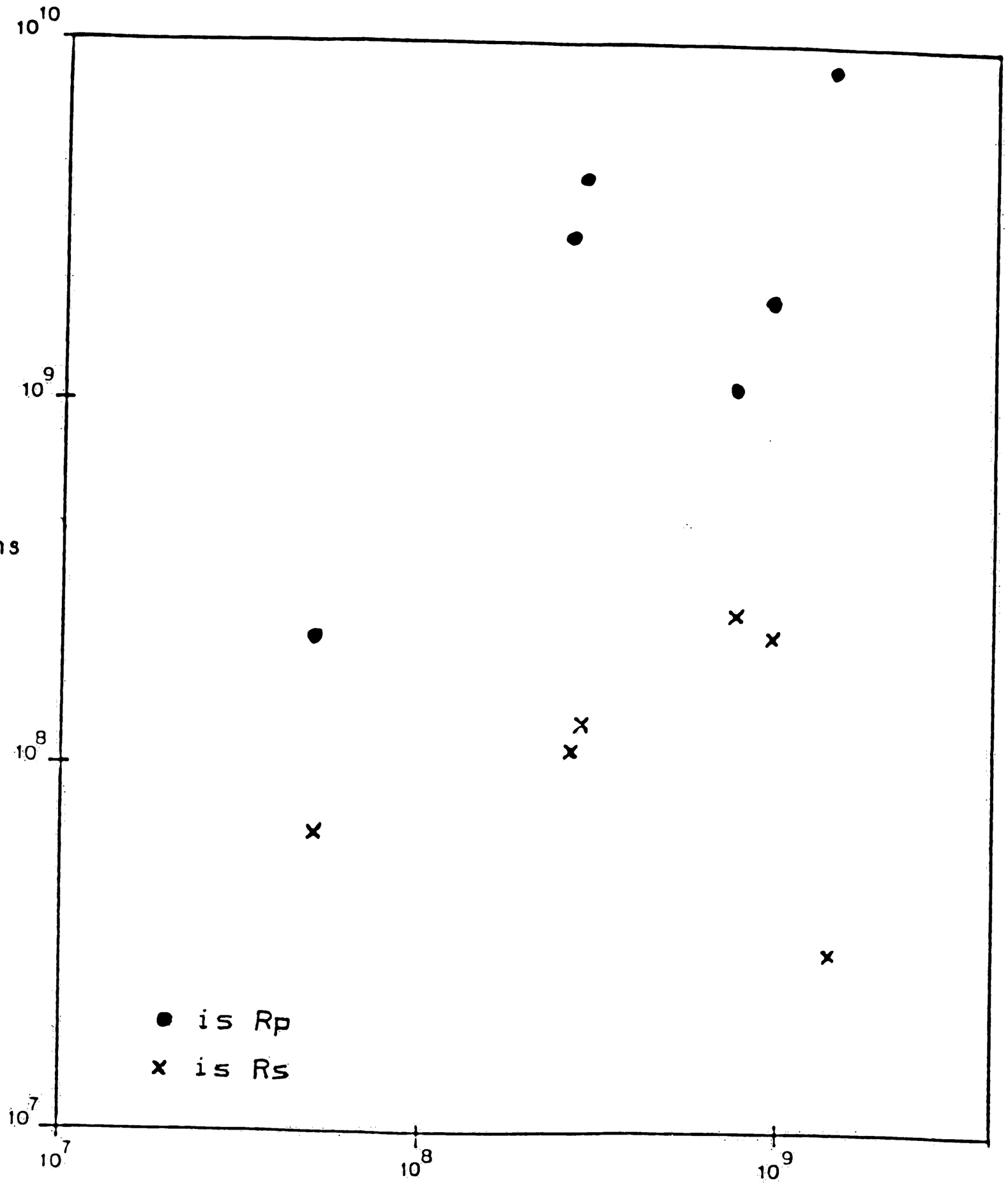

Figure 3.2 Graph of Rp and Rs as a Function of Known Resistivity

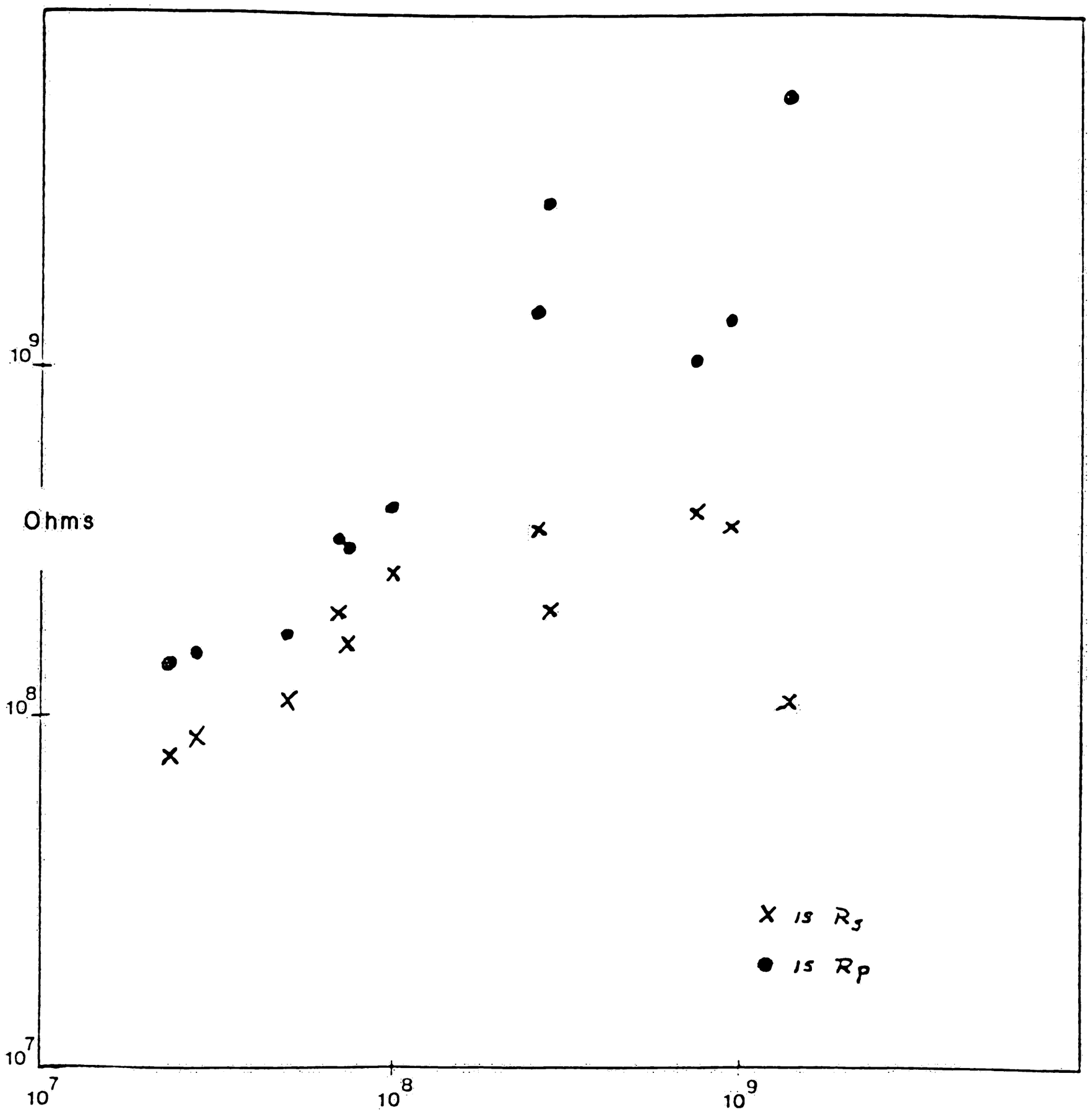

Figure 3.3 Graph of Rp and Rs as a Function of Known Resistivity for Maximum Number of Samples of GaAs

difference. Since the values of Cp are on the order of .3 pF, significant errors are expected. Perhaps a system that is very accurate to fractions of pico-farads would help to place the data on a straight line. Another point of concern is that the samples were tested by different labs to determine their resistivity. It is recommended that one lab test all the samples used in this experiment and use those values obtained as the known values of resistivity. Finally, resistivity across a GaAs wafer can vary by a factor of two. Having one lab test the actual pieces used would also add confidence to the data.

Probe

The details of the probe have been omitted until now. All probes were made by etching away unwanted copper from PC boards. Rectangular geometries were chosen for ease of construction. The operating surface of the probes were two side by side rectangles small enough to be completely covered by the smallest samples. We have no evidence to show that larger samples look different than smaller samples of the same resistivity if the same probe surface is completely covered. Below is a full size drawing of the probe.

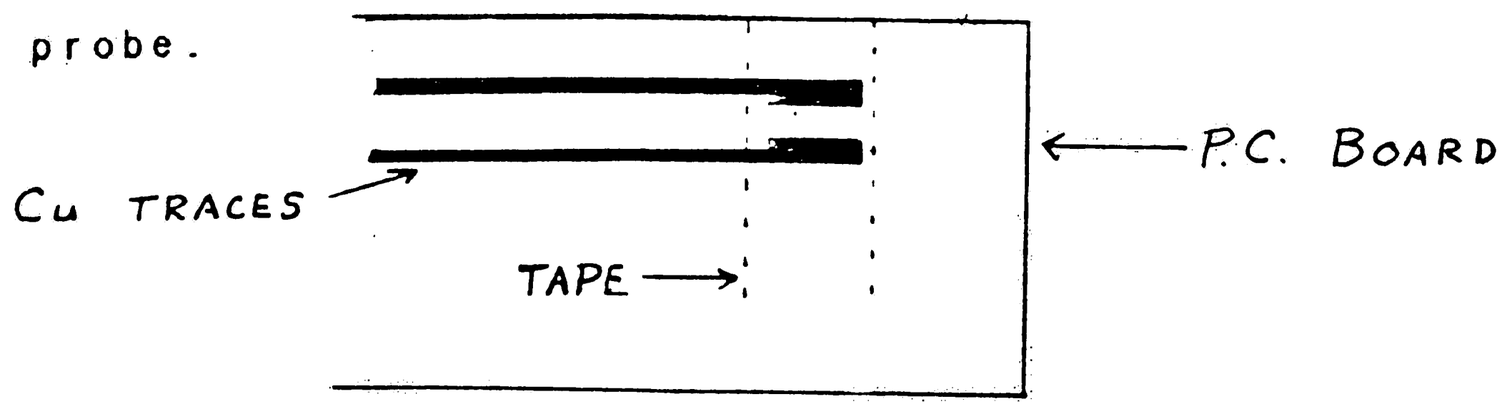

A piece of cellophane tape covers the rectangles. The tape serves both as an insulator and as an index mark to be sure that the same amount of probe is covered by each sample.

A necessary addition to the probe is a nominal piece of twisted pair wire. Figures 3.4a and 3.4b show the outcome for different lengths of wire for the samples of Figure 3.2 . It seems that the twisted pair adds enough capacitance to the probe to enable the meter to give Cp and D readings. As can be seen, the final curves are not significantly different, only Ro has changed. However, the changes in dissipation for different samples are greater for shorter wires. Data indicates that the shortest wires (that still introduce enough capacitance for the meter to operate) cause greater changes in D between any two samples. This should make for a more sensitive instrument that can resolve smaller differences in resistivity.

The final requirement for the probe is that it be on a large metal ground plane and that a similarly grounded box surrounds the probe. This minimizes any effects due to light and rf interference. This shielding is essential to attain stability in the Cp and D readings.

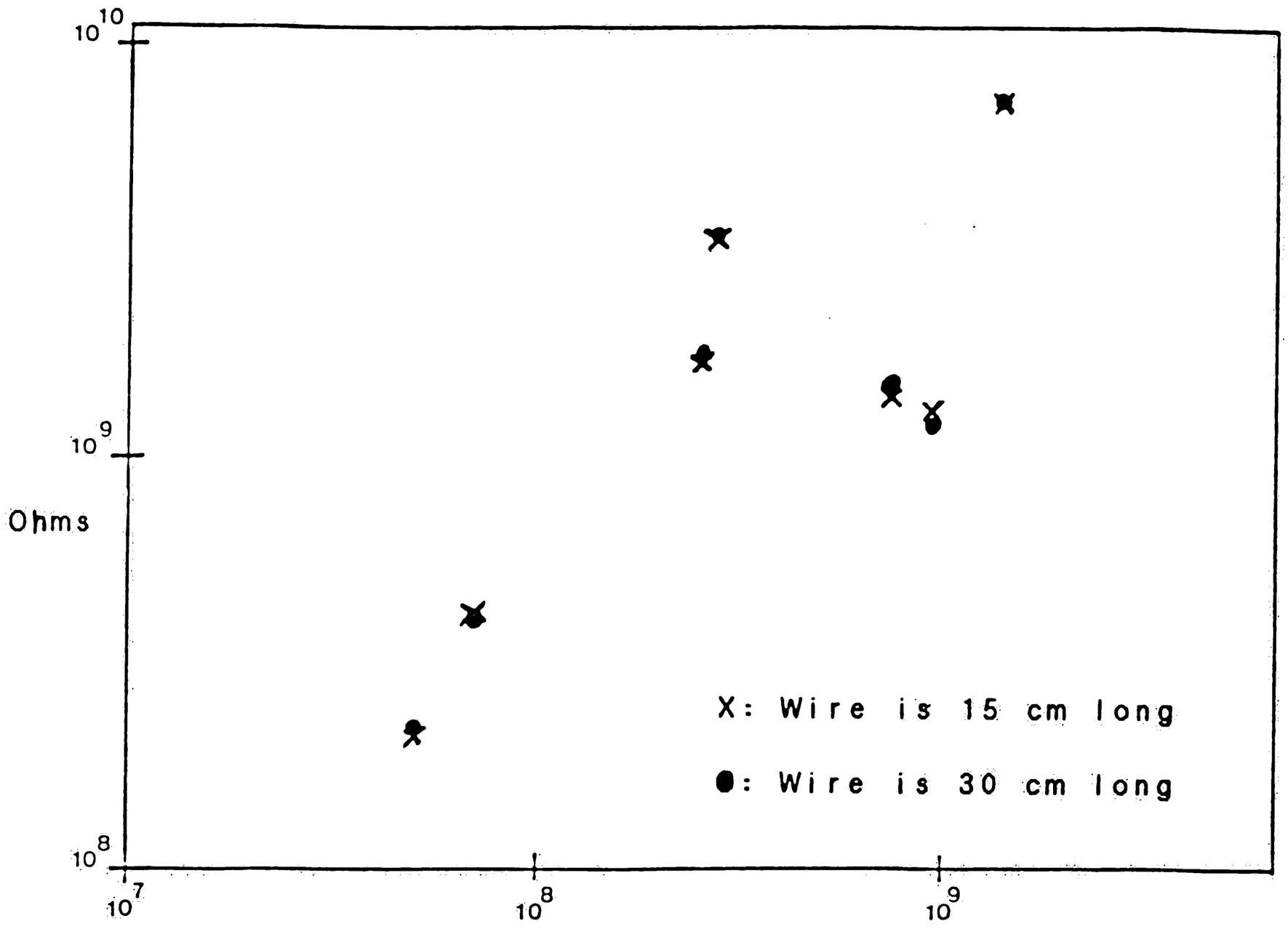

Figure 3.4a Graph of Rp vs Known Resistivity for Different Wire Lengths

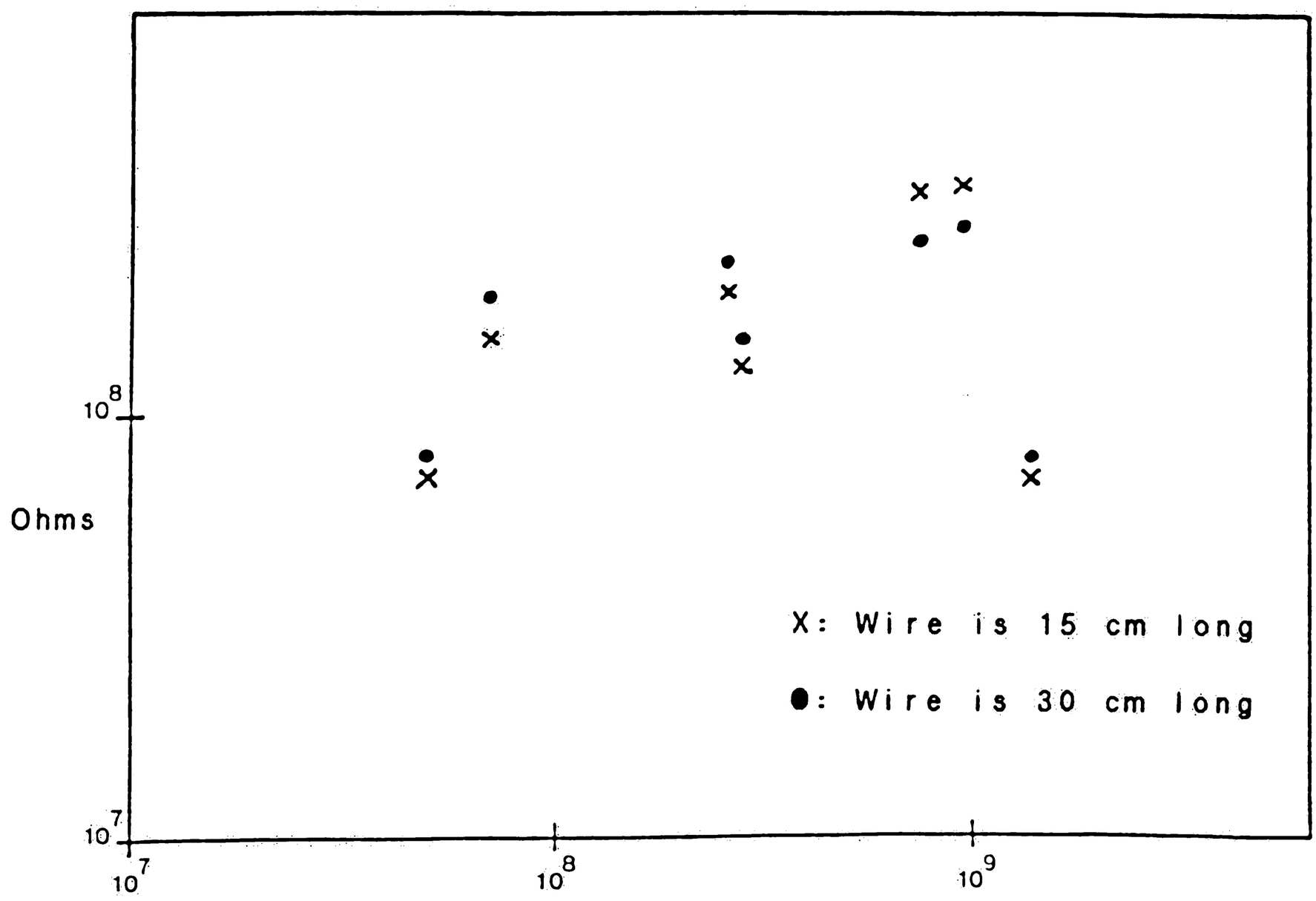

Figure 3.4b Graph of Rs vs Known Resistivity for Different Wire Lengths

CONCLUSION

Three ways to contactlessly determine the resistivity of semiconductors were discussed in this paper. The first method used the semiconductor to load a resonant circuit. The second method used quadrature techniques to find the real (resistive) component of a signal applied to the semiconductor. The last method also used a type of quadrature detection, but used an HP LCR meter to supply the data to calculate the resistivity.

The original resistance measurement technique involved building a quartz crystal controlled oscillator with Automatic Gain Control. The circuit also had the ability to modulate the signal applied to the quartz crystal. Ideally, the high Q of the crystal should drastically attenuate the sidebands. If the Q of the crystal was degraded by putting a capacitive probe loaded with a semiconductor in parallel with the crystal, more sideband energy should be observed depending on the resistivity of the semiconductor. Also the output voltage of the AGC should reflect the amount of energy dissipated by the semiconductor, giving insight to its conductivity.

When the circuit was constructed and

simply loaded by soldering resistors in series with a fixed capacitor (the model for a semiconductor on a capacitance probe), the DC level of the AGC dropped as resistors from 100 ohms to 10K ohms were added. This result was expected. For resistors of 80K up to 900KΩ, the DC output increased as the resistors did. This was not expected. When the series RC was replaced by silicon samples on the probe (the range for the resistors indicated that GaAs could not be observed on by our circuit) the output showed the same trend; the DC level dropped as the resistance increased from 4 ohm-cm to 360 ohm-cm, but then rose for the 755 ohm-cm case. The reason for this rise at the higher resistivities is probably due to the impedance seen after transforming the series model into the equivalent parallel model as shown in Chapter 3.

Monitoring the amount of modulation at the crystal as resistors were soldered across the crystal showed unexpected results. The AC level increased as resistors from 1K were increased to 50KΩ. This is the opposite of what was expected. As resistors were increased from 80KΩ to 10MΩ, the AC level fell as expected. This time the silicon samples were undistinguishable for the 4 and 32 ohm-cm cases. The output then rose as the resistivity went to the 360 and

755 ohm-cm samples.

One factor contributing to the non-ideal behavior observed comes from the characteristics of the quartz crystal. The circuitry was designed to operate the crystal in its parallel mode. The series mode is very close to the parallel mode in the frequency domain. Capacitively loading the crystal changes the parallel resonant frequency, quite possibly to where the low impedance and phase shifts of the series resonant mode can be felt. Capacitively introducing semiconductors to a resonant crystal operating in parallel mode does not seem to be a viable resistivity determining technique, at least not for a large resistivity range.

The second method explained was a quadrature measurement technique. The probe loaded with a semiconductor can be modeled as a resistor in parallel with a capacitor. This can be used as the input to a summing amplifier. The output would consist of a signal inphase with the driving signal due to the resistive part, and a signal 90 degrees out of phase due to the capacitor. If the composite output signal is multiplied by the driving signal and then filtered for DC, the amount of DC is inversely proportional to the

resistance. For discrete resistor-capacitor combinations, the experimental output agreed with the theoretical expectation. When the probe loaded with Si was used, the result looked very similar to the output of the AGC for the first method. The output dropped as expected as the resistance increased to 360 ohm-cm, but then unexpectedly rose for the 755 ohm-cm case. As before, the limited success in the silicon range discouraged even trying GaAs.

A major difficulty with this method was excessive drifting when the probe was used in place of the discrete components. Shielding with metal boxes reduced the output's sensitivity to our physical position somewhat, but not sufficiently to produce accurate results with only one reading. The cumulative errors due to the op-amp offset voltages and currents further aggravated the problem. As a resistivity measuring system, some success is expected for resistances up to 360 ohm-cm. The now characteristic rise for the 755 ohm-cm sample prohibits attempting higher resistivities. One haunting possibility unaddressed until now could be that the 755 ohm-cm sample is misvalued. For the sake of completeness, the four silicon samples should be measured again by conventional accepted means.

The final and most promising method discussed used a common piece of test equipment, straight forward mathematics, and a new model for the probe loaded with a semiconductor. This method shows great potential for GaAs. It does not work with the silicon samples.

The new model for the probe/semiconductor evolved from a series resistor and capacitor to a resistance (Ro) in parallel with a capacitor (Co) in parallel with the original series RC (Rs and Cs respectively). Ro and Co are characteristic of the probe design, wire length and routing, and meter input circuitry. This new model easily transforms into an all parallel model consisting of Ro, Co, Rp and Cp where Rp and Cp relate to Rs and Cs.

The probe is connected to an LCR meter set up to determine capacitance in the parallel mode. Readings for capacitance (C) and dissipation (D) are recorded. To begin the measurement, the probe is unloaded and connected to the meter. The value of Ro is calculated by

$$Ro = \frac{1}{2\pi f C D}$$

where f is the operating frequency of the meter. Co is

simply the capacitance for the probe in its unloaded condition. When samples are placed on the probe, the C and D readings on the meter are Ceq and Req. Rpeq is defined as

$$Rpeq = \frac{1}{2\pi f\ Ceq\ Deq}$$

Solving for Rp gives

$$Rp = Rpeq\ Ro/(Ro-Rpeq)$$

Cp is simply

$$Cp = Ceq - Co$$

Values of Rp and Cp can now be transformed to Cs and Rs data by way of the parameter D. Remember that the D given by the meter is actually Deq. To find the proper D,

$$D = \frac{Ro}{Ro + Rp} * \frac{Ceq}{Co} * Deq$$

Now we find that

$$Rs = \frac{D^2}{1 + D^2}\ Rp$$

Although a straight line was not observed for an Rs vs Resistivity graph, the overall shape is correct. As with the silicon samples, it seems necessary to have the resistivity of all the GaAs samples determined by one recognized laboratory.

Of the three semiconductor resistivity determining methods described, only the LCR meter method seems easily integrated into a viable resistivity measuring instrument for GaAs. The first step would be to use an LCR meter that offered better resolution. In all the experiments, the capacitance was recorded to the nearest 0.05 pF. Dissipation was recorded to the nearest 0.0005. In both cases the "5" in the last decimal place represented that the respective value was fluctuating in the last place given by the meter. A meter that could offer one more decimal place in both dissipation and capacitance could change a final Rp value by as much as 75% in the high resistivity case. That is enough to place all Rp points of Figure 3.3 on a straight line. One further experiment with the higher resolution meter almost seems a necessity.

The quadrature detection method showed limited success in the silicon range of resistivity. The differential scheme showed the noise level in the measurements to be on the order of 30 mV for discrete resistors and capacitors used in place of the semiconductor and probe. When the actual silicon samples and probe were used, the resultant DC output showed differences on the order of 10 mV between the

samples. Better instrumental op-amps could reduce the errors due to offsets and inherent noise, as could better circuit construction and shielding techniques. Better probe design could also help. Smaller working probe surfaces should reduce any rf noise effects and add some stability to the circuits. Overall the quadrature technique appears to be a feasible resistance measurement technique for use with silicon in the 10^{0} to 10^{3} ohm-cm range.

The resonant circuit approach showed the least success for determining resistivity of semiconductors. One aspect not fully investigated is the effect of different probe sizes and geometries. Unfortunately, this method requires the most future work if it is ever going to be a recognized contactless resistivity determining technique.

Bibliography

Articles

Eden, R. C., Livingston, A. R. and Welch, B. M.

"Integrated Circuits: the Case for Gallium Arsenide" IEEE Spectrum, Vol. 20 No. 12 (1983), pp. 30-36.

Miller, G. L., Robinson, A. H., and Wiley, J. D.

"Contactless Measurement of Semiconductor Conductivity by Radio Frequency Free Carrier Power Absorption" Review of Scientific Instruments, Vol. 47, No. 7, (1976), pp. 799-805

Miyamoto, N. and Nishizawa, J. I., "Contactless Measurement of Resistivity of Slices of Semiconductor Materials" Review of Scientific Instruments, Vol. 38, No. 3, (1967), pp. 360-367.

Patents

Miller et al. "Method for the Noncontacting Measurement of the Electrical Conductivity of a Lamella" United States Patent , No. 4,000,458, Dec. 28, 1976

Appendix I

PHASE SHIFTER

To compensate for the resistances in non-ideal capacitors and non-zero output resistances of sources (including op-amps), phase shifters are included in series with the reference input to the multiplier. When Rp = ∞ , the phase shifters are adjusted to make sure that the two input signals to the multiplier are 90 degrees apart. Below is a single stage of the phase shifter circuits as shown in the top left corner of Figure 2.2 .

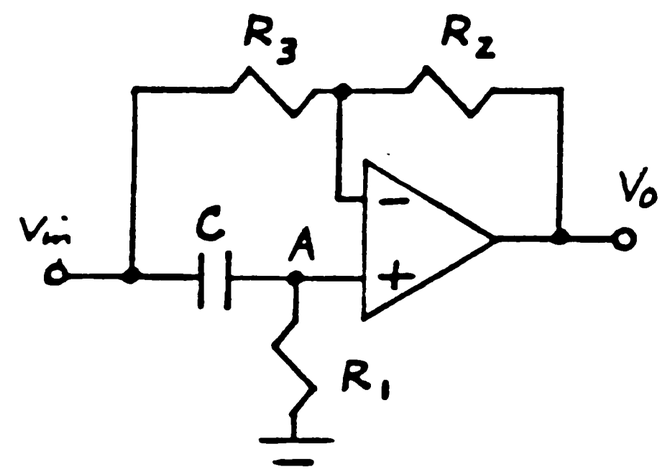

The voltage at node A is

$$Va = Vin \frac{R1}{R1 + 1/(sC)} = \frac{Vin\ (\ sCR1)}{sCR1 + 1}$$

The current flowing through R3 is

$$I3 = \frac{Va - Vin}{R3} = \frac{-Vin}{(sCR1 + 1)\ R3}$$

The current through R2 is

$$I2 = \frac{Vo - Va}{R2} = \frac{Vo\ sC\ R1 + Vo - Vin\ sC\ R1}{(sC\ R1 + 1)\ R2}$$

Assuming no current flows into the inputs of an op-amp, I2 must equal I3. Setting both currents equal and rearranging terms gives

$$\frac{Vo}{Vin} = \frac{sC\ R1\ R3 - R2}{R3} \cdot \frac{1}{sC\ R1 + 1}$$

If R2 = R3 (as it does in Figure 2.2),

$$\frac{Vo}{Vin} = \frac{sC\ R1 - 1}{sC\ R1 + 1}$$

For any w (s = jw), the gain is always unity.

$$|Vo| = \frac{(w\ C\ R1)^2 - 1}{(w\ C\ R1)^2 + 1} |Vin|$$

If R1 is variable, any phase shift from 0 to 180 degrees is possible.

$$\phi = \tan^{-1}(-w\ C\ R1) - \tan^{-1}(w\ C\ R1)$$

The first stage of the phase shifters is used as a coarse adjustment. The phase is adjustable from 11.8 to 97.5 degrees when the operating frequency is 50 Hz.. The second stage is variable from 92.1 to 97.5 degrees. The over-all phase shift is from 103.9 to 195 degrees. Since the input to the phase shifters is ideally 90 degrees, the circuit can advance the phase 15 degrees or retard it 76 degrees if necessary. This is enough to cancel out any undesired phase shifts from non-ideal elements.

Appendix II

LOW PASS FILTER

The low pass filter used (bottom of Figure 2.2) consists of two second order Sallen and Key filters cascaded. A single stage is shown below.

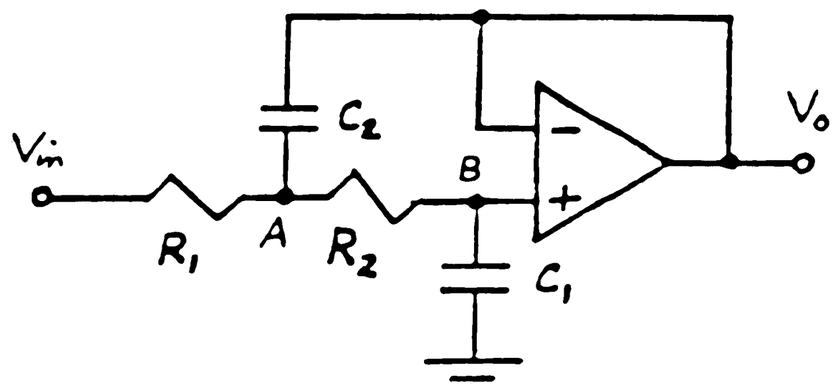

An equation for the current at node B is

$$(1/R2)\ (Vo - Va) + Vo\ sC1 = 0$$

Solving for Va gives

$$Va = Vo(1 + s\ C1\ R2)$$

A similar current equation at node A gives

$$1/R1\ \ (Va - Vin) + 1/R2\ \ (Va - Vo) + (Va - Vo)\ sC2 = 0$$

Substituting for Va and grouping similar terms gives

$$\frac{Vo}{Vin} = \frac{1}{s^2\ R1\ R2\ C1\ C2 + 2s\ C1\ R2 + 1}$$

Solving the transfer function for the frequency at which the output is 0.707, we find the 3 dB point of the first stage to be at 3.1 Hz. The 3 dB point of the second stage is at 0.66 Hz. The signal frequency is 50 Hz.

After the first stage of the low pass filter the signal is down 41 dB. After the second stage it is down an additional 68 dB for a total of 109 dB. Looking at the transfer equation again shows that there is no attenuation for DC.

Appendix III

CALCULATION OF Ro

It is reasonable to assume that the resistance through a material is related to its resistivity by some constant.

$$Rp = k\ p$$

where p is the resistivity of the sample. For identical geometries, k should remain the same as p changes for different samples.

The parallel equivalent resistance derived from the meter readings is

$$Rpeq1 = \frac{Ro\ k\ p1}{Ro + k\ p1}$$

For another sample,

$$Rpeq2 = \frac{Ro\ k\ p2}{Ro + k\ p2}$$

Solving each equation for k and setting them equal gives

$$\frac{1}{p1}\ \frac{Rpeq1}{Ro - Rpeq1} = \frac{1}{p2}\ \frac{Rpeq2}{Ro - Rpeq2}$$

Solving for Ro gives:

$$Ro = Rpeq1\ Rpeq2\ \frac{p2 - p1}{Rpeq1\ p2 - Rpeq2\ p1}$$

Using $p1 = 1.4*10^{9}$ and $p2 = 2.6*10^{8}$, the Ro value obtained this way is within 5% of that derived from the unloaded

probe readings.

Vita

Michael Paul Petroski was born July 7, 1961 of John and Barbara Petroski in Scranton, Pennsylvania. He attended Lehigh University from August 1979 to January 1984 when he received his Bachelor of Science degree in Electrical Engineering. Working as a Research Assistant and Teaching Assistant, he continued his studies at Lehigh University for a Master's Degree in Electrical Engineering (expected in October, 1985). After working as a co-op for IBM in East Fishkill, New York during his undergraduate career, he is now continuing his career with IBM, this time in Boca Raton, Florida as an Electrical Engineer in Automated Packaging and Warehousing.